THE AMERICAN MINERALOGIST, VOL. 56, MAY-JUNE, 1971

COMPOSITION OF THE ANTHOPHYLLITE-GEDRITE SERIES, COMPARISONS OF GEDRITE AND HORNBLENDE, AND THE ANTHOPHYLLITE-GEDRITE SOLVUS

PETER ROBINSON, *Department of Geology, University of Massachusetts, Amherst, Massachusetts, 01002*
MALCOLM ROSS, *U. S. Geological Survey, Washington, D. C. 20242*
AND
HOWARD W. JAFFE, *Department of Geology, University of Massachusetts, Amherst, Massachusetts, 01002*

ABSTRACT

Evaluation of available analyses indicates the anthophyllite-gedrite series is a solid solution between two end compositions

$$\square R^{2+}_2R^{2+}_5Si_8O_{22}(OH)_2 \quad \text{and} \quad Na_{0.5}R^{2+}_2(R^{2+}_{3.5}R^{3+}_{1.5})Si_6Al_2O_{22}(OH)_2$$

where R^{2+} = Mg, Fe^{2+}, Mn^{2+}, Ca, and R^{3+} = Al, Fe^{3+}, $(Ti^{4+}_{1/2}+Fe^{2+}_{1/2})$. A similar evaluation of calcic amphiboles suggests that a high proportion fall in an actinolite-hornblende series between two analogous end compositions

$$\square Ca_2R^{2+}_5Si_8O_{22}(OH)_2 \quad \text{and} \quad Na_{0.6}Ca_2(R^{2+}_{3.6}R^{3+}_{1.4})Si_6Al_2O_{22}(OH)_2.$$

Calcic amphiboles between actinolite and ideal edenite, tschermakite, or pargasite are rare. The apparent coupling of the two coupled substitutions, $Na^{A}Al^{IV}$ for $\square^{A}Si^{IV}$ and $(R^{3+})^{VI}Al^{IV}$ for $(R^{2+})^{VI}Si^{IV}$, and the half-occupied A site implied by the gedrite and hornblende formulae are not readily explained by determined gedrite and hornblende structures.

There is apparently complete solid solution in the anthophyllite-gedrite series at high temperature as demonstrated in specimens from the sillimanite zone of southwestern New Hampshire and Massachusetts. On cooling, members with intermediate Al and Na content exsolved to an anthophyllite-gedrite intergrowth as shown by X-ray single-crystal photographs. Some of the intergrowths are coarse enough so that (010) lamellae of anthophyllite (0.2 μm thick) and gedrite (0.8 μm thick) are visible under the petrographic microscope. Other intergrowths are optically homogeneous but show a strong blue, green, or yellow schiller effect believed to be due to submicroscopic exsolution. Exsolved anthophyllite and gedrite lamellae in the New Hampshire and Massachusetts intergrowths are estimated to contain approximately 0.2 and 1.6 tetrahedral Al respectively. The Fe/Mg ratio is believed to have little influence on the width of the solvus in the composition range of the specimens studied. Under conditions of primary crystallization below the crest of the solvus, as reported by Stout from southern Norway, anthophyllite and gedrite, with tetrahedral Al contents in the ranges 0.29–0.47 and 1.13–1.50 respectively, formed together as two physically separable phases which subsequently underwent no fine-scale exsolution.

Minerals of the anthophyllite-gedrite series occur with other minerals in a wide variety of assemblages. The presence of a primary anthophyllite-gedrite solvus further complicates an already complex set of metamorphic facies types.

INTRODUCTION

New analytical information (Robinson and Jaffe, 1969a, b) has brought to attention the importance of Na in gedrite and the similarity of gedrite,

in many of its chemical characteristics, to hornblende. X-ray single crystal photographs of some analyzed anthophyllites and gedrites from central Massachusetts and southwestern New Hampshire (Robinson, Jaffe, Klein, and Ross, 1969; Ross, Papike, and Shaw, 1969) show that some optically homogeneous amphibole crystals are made up of a microscopic or submicroscopic intergrowth of two orthorhombic amphiboles. Stout (1969, 1970a,b) reported two coarse coexisting orthorhombic amphiboles from Norway differing in their Al and Na content. In view of these findings and the recently completed structure determination on the most aluminous and most sodic gedrite known from southwestern New Hampshire (Papike and Ross, 1970), it seemed worthwhile to examine thoroughly the composition field of the anthopyllite-gedrite series, the crystal chemical relationships between gedrite and hornblende, and the significance of the anthophyllite-gedrite solvus.

Coupled Substitutions in Amphiboles

Compositional variations in amphiboles are most easily conceived in terms of substitutions into two basic amphibole formulae, the clinoamphibole, tremolite,

$$\square^{A}Ca_2{}^{M(4)}Mg_5{}^{VI}Si_8{}^{IV}O_{22}(OH)_2,$$

and the orthoamphibole, anthophyllite,

$$\square^{A}Mg_2{}^{M(4)}Mg_5{}^{VI}Si_8{}^{IV}O_{22}(OH)_2.$$

Simple substitutions of Fe^{2+} and Mn^{2+} for Mg give wide compositional variations, and replacement of Ca of tremolite by Fe^{2+}, Mn^{2+}, and some Mg leads to the compositionally simple cummingtonite series. More complex compositions are derived by four basic coupled substitutions involving Na and Al. When carried to their limit these coupled substitutions lead to idealized end members commonly mentioned in the literature (Ernst, 1968). Where octahedral Al is present it may be replaced by Fe^{3+}, leading to the ferric end members listed in italics. Na in the *A* site may be partially replaced by K.

	Edenite
(1) $Na^{A}Al^{IV}$ for $\square^{A}Si^{IV}$	$Na\ Ca_2\ Mg_5\ Si_7Al\ O_{22}(OH)_2$
	– – – – (orthorhombic)
	$Na\ Mg_2\ Mg_5\ Si_7Al\ O_{22}(OH)_2$
	Tschermakite (*Ferritschermakite*)
(2) $Al^{VI}Al^{IV}$ for $Mg^{VI}Si^{IV}$	$\square Ca_2\ Mg_3Al_2\ Si_6Al_2\ O_{22}(OH)_2$
	Gedrite
	$\square Mg_2\ Mg_3Al_2\ Si_6Al_2\ O_{22}(OH)_2$
	Glaucophane (*Magnesioriebeckite*)

(3) $Na^{M(4)}Al^{VI}$ for $Ca^{M(4)}Mg^{VI}$ $\square Na_2\ Mg_3Al_2\ Si_8\ O_{22}(OH)_2$

Richterite

(4) $Na^{A}Na^{M(4)}$ for $\square^{A}Ca^{M(4)}$ $Na\ CaNa\ Mg_5\ Si_8\ O_{22}(OH)_2$

Combinations of these basic coupled substitutions lead to other ideal end members, named and unnamed.

Pargasite (*Magnesiohastingsite*)

(5) Substitutions 1) and 2) $Na\ Ca_2\ Mg_4Al\ Si_6Al_2\ O_{22}(OH)_2$

– – – – – (orthorhombic)

$Na\ Mg_2\ Mg_4Al\ Si_6Al_2\ O_{22}(OH)_2$

Eckermannite (*Magnesioarfvedsonite*)

(6) Substitutions 3) and 4) $Na\ Na_2\ Mg_4Al\ Si_8\ O_{22}(OH)_2$

"Barroisite" (Binns, 1967)

(7) Substitutions 2) and 3) $\square CaNa\ Mg_3Al_2\ Si_7Al\ O_{22}(OH)_2$

– – – – (Phillips and Layton, 1964)

(8) Substitutions 1) and 3) $Na\ Na_2\ Mg_3Al_2\ Si_7Al\ O_{22}(OH)_2$

– – – – (*Katophorite* with Fe^{2+})

(9) Substitutions 3) and 4) $Na\ CaNa\ Mg_4Al\ Si_7Al\ O_{22}(OH)_2$

– – – – (Phillips and Layton, 1964; *Mbozite* with Fe^{2+})

$Na\ CaNa\ Mg_3Al_2\ Si_6Al_2\ O_{22}(OH)_2$

Ti^{4+} substitutes in the octahedral positions in the same way as Al or Fe^{3+} in substitutions 2) or 3), but each Ti ion requires twice as much compensation as a trivalent ion. Thus, so far as the compensation mechanism is concerned, one Ti^{4+} ion has the equivalent effect of two trivalent ions. Li^{1+} substitutes in octahedral positions probably by the coupled substitution Li Al for Mg Mg.

Sodium Content of Analyzed Anthophyllites and Gedrites

The ion contents per 23 oxygens for seven wet chemical analyses and one electron probe analysis of anthophyllites and gedrites from New Hampshire and Massachusetts are given in Table 1. These analyses are plotted in terms of Na+K and tetrahedral Al content in Figure 1 along with the results of eleven other electron probe analyses from the same area (Klein, 1968; Robinson and Jaffe, 1969b, Table 4). None of the analyses even approximates the ideal sodium-free gedrite formula given in recent summaries of amphibole compositions (Deer, Howie, and Zussman, 1963; Ernst, 1968). The ratio of Na+K to tetrahedral Al is remarkably constant. It is not 1/1 as would be consistent with an edenite-

TABLE 1. IONS PER 23 OXYGENS FOR ANTHOPHYLLITES AND GEDRITES FROM SOUTHWESTERN NEW HAMPSHIRE AND CENTRAL MASSACHUSETTS[a]

	I34I	I34JX	I38DX	E	W95JX	N30X	6A9X	QB27C-2B[b]
Si	5.950	6.396	6.557	6.686	6.683	7.176	7.314	7.53
P	.005	.009	.007	.007	.002	.002	.002	—
Al	2.045	1.595	1.436	1.307	1.315	.822	.684	.47
$\sum$ (tet.)	8.000	8.000	8.000	8.000	8.000	8.000	8.000	8.00
Al	1.364	1.011	1.010	1.014	.892	.504	.461	.47
Fe^{3+}	.133	.260	.141	.035	.168	.098	.127	—
Cr^{3+}	.002	—	—	—	.002	.007	.002	—
Ti^{4+}	.027	.050	.033	.063	.025	.021	.025	—
Mg	3.005	3.557	3.148	4.142	4.320	4.439	3.953	4.11
Li	.018	.022	.035	—	.005	.005	.012	—
Ni	—	—	.001	—	.001	.006	.002	—
Fe^{2+}	2.355	1.899	2.453	1.567	1.415	1.758	2.132	2.25
Mn^{2+}	.031	.045	.042	.017	.026	.043	.091	.06
Ca	.042	.071	.053	.086	.083	.113	.112	.06
Na	.023	.085	.084	.076	.063	.006	.083	.05
$\sum$ (M-sites)	7.000	7.000	7.000	7.000	7.000	7.000	7.000	7.00
Na	.521	.322	.325	.176	.274	.180	.135	.05
K	.007	.002	.003	.005	—	—	.003	—
$\sum$ (A-site)	.528	.324	.328	.181	.274	.180	.138	.05
H	2.611[c]	2.013	2.394	2.292	1.982	2.308	2.301	—
F	.004[c]	.040	.010	—	.018	—	.014	—
FeO+MnO/FeO +MnO+MgO	.44	.35	.44	.27	.25	.28	.35	.36

[a] These are the same analyses, except for QB27C-2B, presented in Robinson and Jaffe, 1969b, Table 2, but are calculated on the basis of 23 (O) instead of 24 (O,OH). Analysis E was done in 1892. The rest are recent.

[b] Electron probe analysis (Robinson and Jaffe, 1969b, Table 4), calculated on basis of 23 (O).

[c] Summation to 23 (O) does not include H_2O or oxygen equivalent of F.

like substitution, nor 1/2 consistent with a pargasite-like substitution, but lies close to 1/4. Thus, for each 0.1 Na ion per formula unit there are 0.4 tetrahedral Al ions substituting for Si, the charge deficiency caused by the additional 0.3 tetrahedral Al ions being compensated by substitution of Al^{3+}, Fe^{3+}, or Ti^{4+} for Mg^{2+} or Fe^{2+} in the octahedral positions. Such a scheme of substitution would lead to an ideal end composition closely approximated by the composition of gedrite I34I:

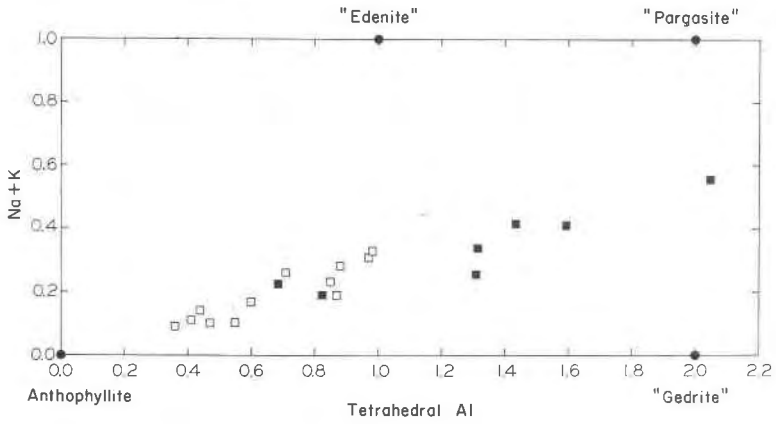

FIG. 1. Plot of Na+K and tetrahedral Al per 23(O) for 7 wet analyzed (closed squares) and 12 electron probe analyzed (open squares) anthophyllites and gedrites from New Hampshire and Massachusetts (see text). Positions of some ideal amphibole end members are indicated.

$$Na_{0.5}(Mg, Fe^{2+})_2(Mg, Fe^{2+})_{3.5}Al_{1.5}Si_6Al_2O_{22}(OH)_2$$

Other analyses of anthophyllites and gedrites (Appendix) are plotted in the same manner in Figure 2 using the ion contents per formula unit calculated by the various authors. These analyses show a relationship similar to that of Figure 1 with somewhat more scatter due to quality of

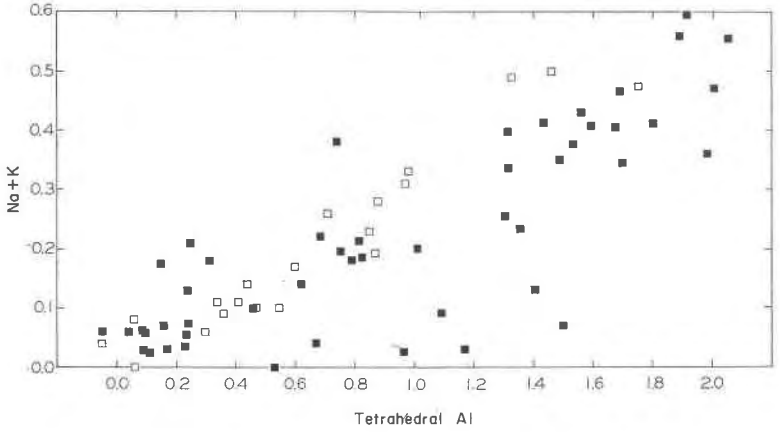

FIG. 2. Plot of Na+K and tetrahedral Al per formula unit for published anthophyllite-gedrite analyses (see appendix) including those in Figure 1. Closed squares, wet analyses; open squares, probe analyses. Analyses with less than 0.0 tetrahedral Al contain greater than 8.00 Si.

analyses, and the fact that most are calculated on the basis of 24(O, OH). With this indication that anthophyllites and gedrites generally show a similar relationship of Na+K and tetrahedral Al, a more rigorous evaluation and characterization of analyses seemed in order.

Structural Formulae of Anthophyllites and Gedrites

The analyses in Table 1 suggest a solid solution series between anthophyllite $\square R^{2+}{}_2R^{2+}{}_5Si_8O_{22}(OH)_2$ and gedrite $Na_xR^{2+}{}_2$ $(R^{2+}{}_{5-y}R^{3+}{}_y)$ $(Al_{x+y}Si_{8-x-y})$ O_{22} $(OH)_2$where Na occupies the otherwise vacant A site, R^{2+} = Mg, Ni, Fe^{2+}, Mn,Ca; R^{3+} = Al+Fe^{3+}+Cr^{3+}+($Ti^{4+}{}_{1/2}$+$R^{2+}{}_{1/2}$); x = A-site occupancy; and y = sum of Al^{VI}+Fe^{3+}+Cr^{3+}+2 Ti^{4+}. In the two important substitution mechanisms of the formula, the substitutions of Na (and K) in the A site (x) and of R^{3+} in the octahedral sites (y) are compensated by substitution of Al for Si in the tetrahedral sites, so that the sum of x and y must be equal to the amount of tetrahedral Al as shown in the ideal formula. A difference between (x+y) and tetrahedral Al for an analysis (residual value) would indicate a substitution not described by the ideal formula, or analytical errors. Evaluations of eight analyzed anthophyllites with reference to the ideal formula are given in Table 2. Small deviations from the ideal formula are shown by the small residual values listed in column 5. A positive residual could indicate an addiotinal glaucophane-like or richterite-like substitution, or analytical errors. A negative residual could be due to an amount of Na+K less than the calculated A-site occupancy, leading to substitution of divalent cations in the A site, or to errors.

Table 2. Idealized Formula for Gedrite and Comparison of Analyses on the Basis of this Formula

$Na_xR^{2+}{}_2(R^{2+}{}_{5-y}R^{3+}{}_y)(Al_{x+y}Si_{8-x-y})O_{22}(OH)_2$

where x = A occupancy and y = octahedral Al+Fe^{3+}+Cr^{3+}+2Ti^{4+}

	(1) x	(2) y	(3) $x+y$	(4) Al^{IV}	(5) [a]$(x+y)$-Al^{IV}	(6) x/Al^{IV}	(7) $x/(x+y)$
I34I	.53	1.55	2.08	2.05	+.03	.26	.25
I34JX	.32	1.37	1.69	1.60	+.09	.20	.19
I38DX	.33	1.22	1.55	1.44	+.11	.23	.21
W95JX	.27	1.11	1.37	1.32	+.05	.20	.20
E	.18	1.18	1.36	1.31	+.05	.14	.13
N30X	.18	.65	.83	.82	+.01	.22	.22
6A9X	.14	.64	.78	.68	+.10	.21	.18
QB27C-2B[b]	.05	.47	.52	.47	+.05	.11	.10

[a] "Residual value."

[b] Probe analysis.

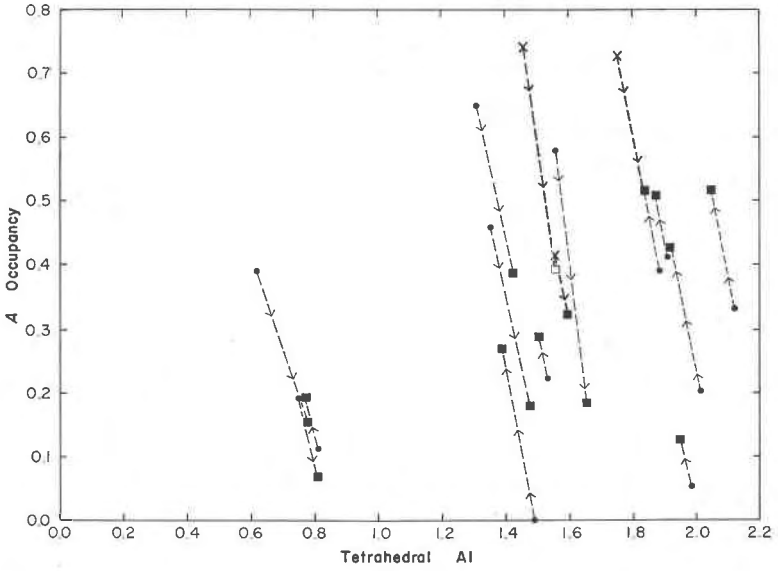

FIG. 3. Effect of recalculation scheme and Fe_2O_3 content on calculated A-site occupancy and tetrahedral Al for selected anthophyllites and gedrites (see appendix). Closed circle, wet analysis calculated on basis of 24(O,OH); closed square, wet analysis calculated on basis of 23(O); open square, probe analysis recalculated with correction for assumed Fe_2O_3 content; X, wet or probe analysis calculated on basis of 23(O) with total Fe as FeO. Wet analyses displaced upward by recalculation to 23(O) have high H_2O analyses, those displaced downward have low H_2O analyses. Assumption of total Fe as FeO results in higher calculated A-site occupancy.

For analyses that agree with the ideal formula a complete range in the relative values of x and y or the ratios x/tetrahedral Al and $x/(x+y)$ is possible. However, with the exception of E, which is an old analysis, and QB27C-2B, which is a probe analysis, the analyses in Table 2 (columns 6 and 7) show a very limited range for these values between 0.18 and 0.26.

Published anthophyllite and gedrite analyses were compared using the method outlined above. Residual values proved to be very large for many published structural formulae calculated on the basis of 24(O,OH), but very small when recalculated on the basis of 23(O). The strong effect of erroneous H_2O determinations on the calculated A-site occupancy is graphically demonstrated in Figure 3. These results gave justification for the recalculation of all analyses on the basis of 23(O). The effect on A occupancy of an erroneous ferric iron determination, or the assumption that all iron is ferrous, as in the case of microprobe analyses, is also shown for three analyses in Figure 3. Underestimation of the amount of Fe_2O_3 results in overestimation of the proportion of cations to oxygen in the

structure. This in turn results in an extra high calculated A-site occupancy, including the assignment of Ca or even Mn, Fe, or Mg to the A site, which seems improbable but not impossible on crystal-chemical grounds (J. J. Papike, pers. comm. 1969), except where Be^{2+} occupies adjacent tetrahedra (Moore, 1969). This high calculated A-site occupancy further results in a ratio of A occupancy to tetrahedral Al which falls far off the trend shown by the wet analyses (Fig. 4). Indeed, if one were to assume that the trend is linear and all analyses should fall on it, one can calculate the amount of Fe^{3+} required to correct an electron probe

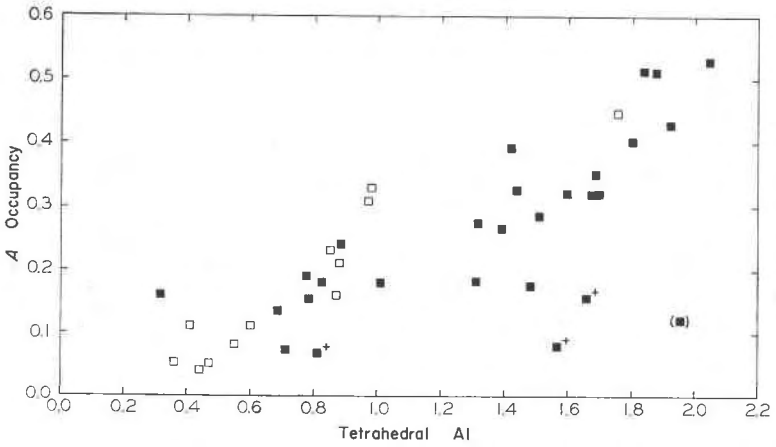

FIG. 4. A-site occupancy against tetrahedral Al for published anthophyllite-gedrite analyses (see appendix) calculated on basis of 23(O) per formula unit and satisfying other criteria given in text. Closed squares, wet analyses; open squares, probe analyses; brackets, analysis of Seki and Yamasaki (1957, see text); crosses, analyses in Rabbitt (1948, see text).

analysis and bring it onto the linear trend. To limit further the effect of possible analytical errors in the consideration of A occupancy and tetrahedral Al, analyses were considered only if their recalculation to 23(O) showed tetrahedral Al greater than the arbitrarily chosen value of 0.3, and an A site occupied by Na and K, and negligible or no Ca.

The A occupancies and tetrahedral Al contents for 32 published analyses and the eight analyses given in Table 1 are shown in Figure 4. The high alumina gedrite (in brackets in Fig. 4), which shows low A occupancy and a high residual, is the ferrogedrite of Seki and Yamasaki (1957) which was corrected for 6 percent chlorite impurity in the sample. The three low A occupancy gedrites that are marked by crosses, are all from Rabbitt (1948), and were analyzed by the same analyst. The re-

maining points form a clear substitution trend, in which the ratio of *A*-site occupancy to tetrahedral Al is near 1/4 or 1/5, and there is a coupling of two coupled substitutions $Na^{A}Al^{IV}$ for $\square Si^{IV}$ and $(R^{3+})^{VI}Al^{IV}$ for $(R^{2+})^{VI}Si^{IV}$ in a ratio of 1/3 or 1/4.

Comparison of Orthorhombic Amphiboles and Calcic Clinoamphiboles

At one stage in the evaluation of analyses it occurred to the authors to use the residual value (column 5, Table 2) as a coordinate in a plot against the ratio $x/(x+y)$ (Fig. 5). When all orthorhombic amphibole formulae were recalculated to 23 oxygens, most large residuals disappeared, but the method of plotting in Figure 5 proved useful, as will be seen below. This type of diagram illustrates what might be called the "big bang" theory of amphiboles. It shows approximately the *direction* in which the amphibole analyses depart from the ideal end members anthophyllite or tremolite, but not the amount of this departure. It is interesting to see (Table 3, columns 5 and 7) how some other ideal amphibole end members would plot on such a diagram. One group of members, tschermakite, pargasite, and edenite has a residual of 0; a second group, "barroisite," katophorite, and richterite has a residual of 1, and a third group, glaucophane and eckermannite has a residual of 2. A large positive residual value is due to Na in the $M(4)$ position compensated by trivalent octahedral ions or by Na in the A site. There seems to be a lack of suggested ideal end members that have a negative residual value, although an amphibole with the A site occupied by Ca would show a negative value. Because all large positive residuals are due to Na occupancy in $M(4)$ (Table 3), it is obvious why anthophyllites and gedrites do not have a substantial residual. The orthorhombic amphibole structure is one characterized by a small $M(4)$ site containing small cations such as Mg and Fe^{2+}. The $M(4)$ site in orthoamphiboles thus cannot accommodate significant amounts of the large Na ions as can clinoamphiboles. Nevertheless, the small positive residuals shown by many of the analyses in Figure 5, with a cluster near $+0.1$, suggest a small amount of Na in $M(4)$ as a glaucophane component, a suggestion supported by the analyses in Table 1.

An obvious next step was to apply the same criteria to calcic clinoamphiboles. For this purpose the compilation of Leake (1968) was extremely convenient and was supplemented by analyses from Binns (1965, 1967); Dodge, Papike, and Mays (1968); Henderson (1968); Robinson and Jaffe (1969b); and a few chemically extreme types from Deer, Howie, and Zussman (1963). All of the analyses in Leake's compilation as well as those of Deer, Howie, and Zussman are calculated to 24(O,OH). Because the labor of recalculating these would have been

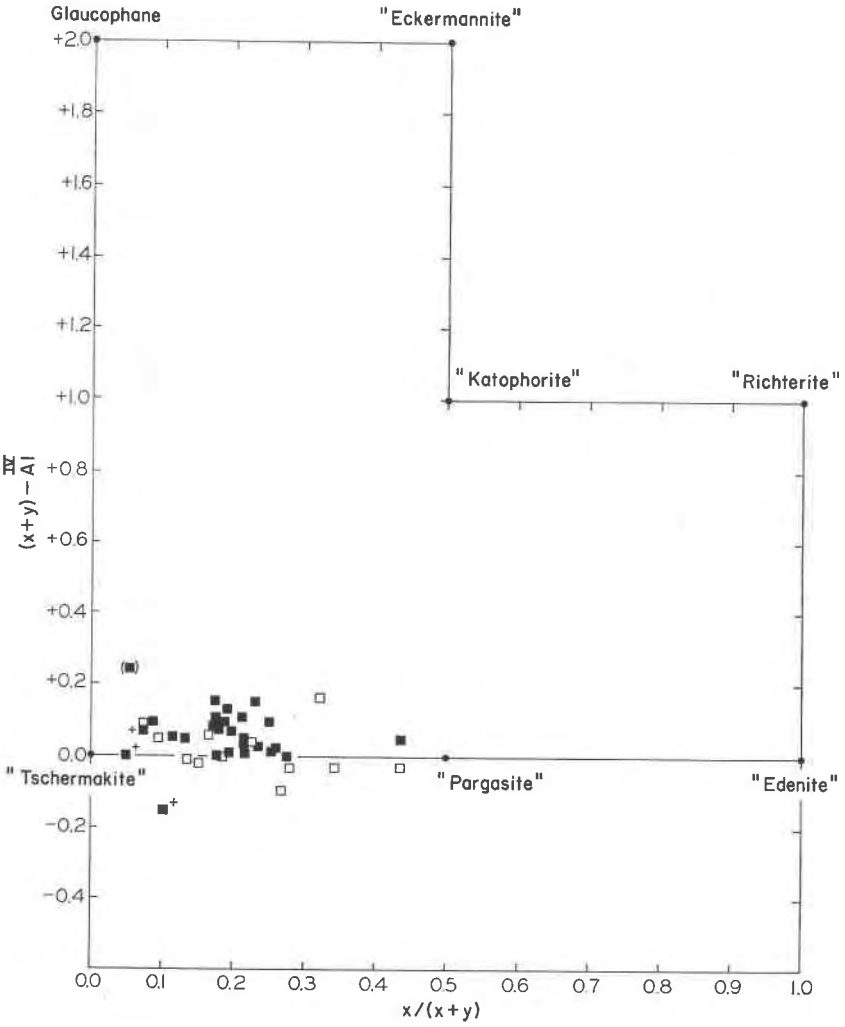

FIG. 5. Analyzed anthophyllites and gedrites (see Fig. 4) plotted on the basis of the residual value, $(x+y)$-Al^{IV}, and the ratio $x/(x+y)$. Positions of some ideal amphibole end members are shown on the same basis for comparison. Symbols have same meaning as in Figure 4.

enormous, only analyses with (OH) closely approaching 2.00 were used for comparison because only those have ion contents close to contents calculated on the basis of 23(O). In practice analyses with OH per 24(O,OH) between 1.80 and 2.20 were used. Further requirements were that tetrahedral Al had to be greater than an arbitarily chosen value of

TABLE 3. IDEAL CLINOAMPHIBOLE MEMBERS CHARACTERIZED ACCORDING TO IDEAL FORMULA IN TABLE 2

	A	*M*(4)	*M*(1–3)	*T*		(1) x	(2) y	(3) $x+y$	(4) Al^{IV}	(5) $(x+y)-Al^{IV}$	(6) $\frac{(x+y)-Al^{IV}}{(x+y)}$	(7) $x/(x+y)$
1. Tschermakite	□	Ca_2	Mg_3Al_2	Si_6Al_2	$O_{22}(OH)_2$	0.0	2.0	2.0	2.0	0.0	0.0	0.0
2. Pargasite	Na	Ca_2	Mg_4Al	Si_6Al_2	$O_{22}(OH)_2$	1.0	1.0	2.0	2.0	0.0	0.0	0.5
3. Edenite	Na	Ca_2	Mg_5	Si_7Al	$O_{22}(OH)_2$	1.0	0.0	1.0	1.0	0.0	0.0	1.0
4. "Barroisite"	□	CaNa	Mg_3Al_2	Si_7Al	$O_{22}(OH)_2$	0.0	2.0	2.0	1.0	+1.0	+0.5	0.0
5. Katophorite	Na	CaNa	$Fe^{2+}{}_4Fe^{3+}$	Si_7Al	$O_{22}(OH)_2$	1.0	1.0	2.0	1.0	+1.0	+0.5	0.5
6. Richterite	Na	CaNa	Mg_5	Si_8	$O_{22}(OH)_2$	1.0	0.0	1.0	0.0	+1.0	+1.0	1.0
7. Glaucophane	□	Na_2	Mg_3Al_2	Si_8	$O_{22}(OH)_2$	0.0	2.0	2.0	0.0	+2.0	+1.0	0.0
8. Eckermannite	Na	Na_2	Mg_4Al	Si_8	$O_{22}(OH)_2$	1.0	1.0	2.0	0.0	+2.0	+1.0	0.5
9. ? (Phillips and Layton, 1964)	Na	Na_2	Mg_3Al_2	Si_7Al	$O_{22}(OH)_2$	1.0	2.0	3.0	1.0	+2.0	+0.66	0.33
10. ? (Phillips and Layton, 1964)	Na	CaNa	Mg_3Al_2	Si_6Al_2	$O_{22}(OH)_2$	1.0	2.0	3.0	2.0	+1.0	+0.33	0.33
11.	□	CaNa	Mg_4Al	Si_8	$O_{22}(OH)_2$	0.0	1.0	1.0	0.0	+1.0	+1.0	0.0
12.	□	CaNa	Mg_3Al_2	Si_7Al	$O_{22}(OH)_2$	0.0	2.0	2.0	1.0	+1.0	+0.5	0.0
13.	Na	CaNa	Mg_4Al	Si_7Al	$O_{22}(OH)_2$	1.0	1.0	2.0	1.0	+1.0	+0.5	0.5
14.	$Na_{.5}$	CaNa	$Mg_{4.5}Al_{.5}$	Si_8	$O_{22}(OH)_2$	0.5	0.5	1.0	0.0	+1.0	+1.0	0.5
15.	$Na_{.5}$	$Ca_{1.5}Na_{.5}$	Mg_5	Si_8	$O_{22}(OH)_2$	0.5	0.0	0.5	0.0	+0.5	+1.0	1.0
16.	Na	$Ca_{1.5}Na_{.5}$	Mg_5	$Si_{7.5}Al_{.5}$	$O_{22}(OH)_2$	1.0	0.0	1.0	0.5	+0.5	+0.5	1.0

0.3 (with the exception of a few sodic examples), that the sum of Si and tetrahedral Al had to be essentially 8, that the A-site occupancy had to be greater than 0, and that the sum of Na and K had to be greater than or equal to the A-site occupancy. This last rule essentially excluded all structural formulae in which Ca, Mn, or Fe^{2+} is assigned to the A site. Altogether 349 analyses qualified in the way described. The result of this "buckshot" approach is shown on Figure 6. In addition, four hornblende-glaucophane pairs given by Himmelberg and Papike (1969) are shown, to suggest the limit of the hornblende field in the direction of glaucophane under low temperature, high pressure conditions.

Plots such as Figures 5 and 6 usefully portray the calculated Na occupancy of $M(4)$. However, consideration of three pairs of hypothetical formulae at the bottom of Table 3 (Nos. 11–16), shows that the coordinates (columns 5 and 7) do not unambiguously define the *direction* of departure of the structural formula from the ideal tremolite or anthophyllite formula. However, by dividing the residual value (column 5) by the sum of $(x+y)$ a new parameter is derived, $[(x+y)-Al^{IV}]/(x+y)]$, which does uniquely define the direction of departure (column 6). This has the further advantage that the resulting plot against $x/x+y$ (column 7) forms a square that has the characteristics of a ternary reciprocal system (Fig. 7). The four ideal end members, tschermakite ($Al^{VI}Al^{IV}$ substitution, coordinates 0.0, 0.0), edenite ($Na^{A}Al^{IV}$ substitution, coordinates 0.0, 1.0), glaucophane ($Na^{M(4)}Al^{VI}$ substitution, coordinates 1.0, 0.0) and richterite ($Na^{A}Na^{M(4)}$ substitution, coordinates 1.0, 1.0) form the apices of the square. This square has the properties of a projection from the tremolite apex of an amphibole composition polyhedron such as those constructed by Smith (1959), Phillips (1966), Zussman (in Whittaker, 1968) and Whittaker (1968). In addition to tremolite, tschermakite, edenite, glaucophane, and richterite apices, these amphibole polyhedra have apices at pargasite, eckermannite, $NaNa_2Mg_3Al_2(Si_7Al)O_{22}(OH)_2$ (Phillips and Layton, 1964) and $NaNaCaMg_3Al_2(Si_6Al_2)O_{22}(OH)_2$ (Phillips and Layton, 1964), all of which are shown in projection in Figure 7 and listed in Table 3.

The pattern of analyses in Figures 6 and 7 is striking and unexpected on the basis of other published discussions. A large number of analyses falls close to the line tschermakite-pargasite-edenite but analyses that agree closely with these particular substitutions are few. The scarcity of ideal "tschermakite" has already been discussed by Leake (1965) and is well shown. Of the three analyses that fall closest to an "edenite" substitution, one is a synthetic fluoramphibole, the second is a synthetic fluoramphibole with boron in place of aluminum, and the third is an average of two amphibole analyses. Other amphiboles called "edenite"

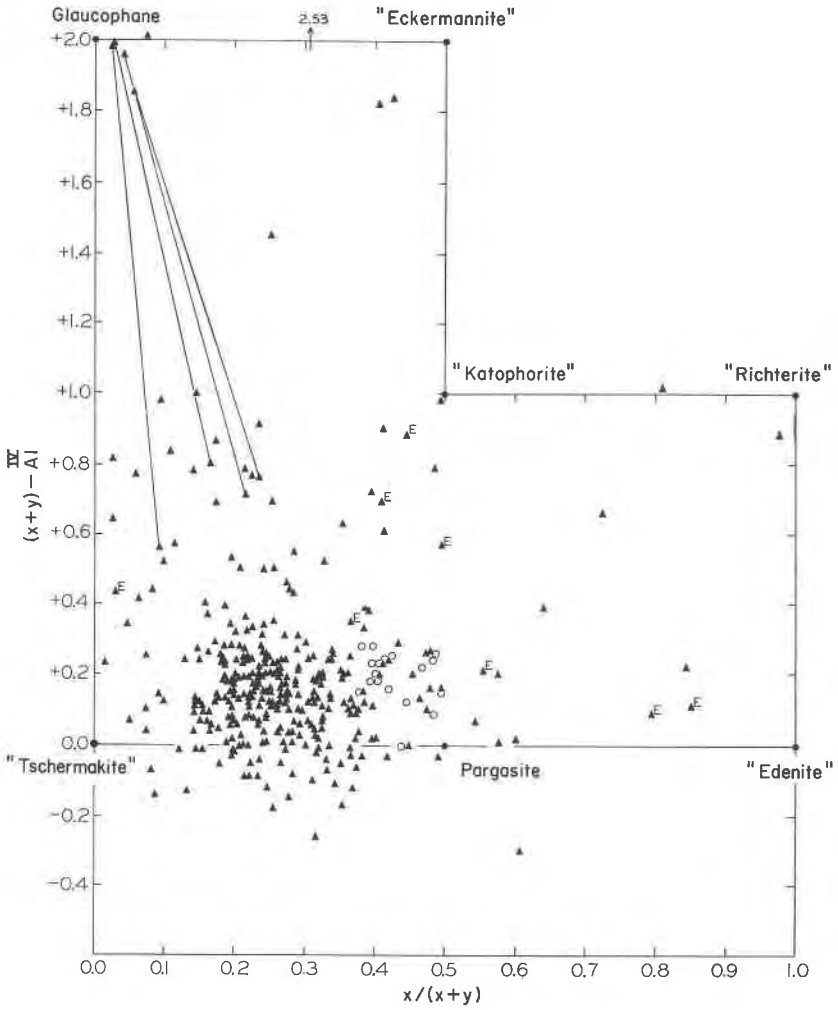

FIG. 6. Plot of 349 clinoamphibole analyses (closed triangles, see appendix), on same basis as Figure 5. Circles indicate potassic hastingsites from Rhodesia (Henderson, 1968); E indicates amphibole described as edenite or edenitic hornblende by Leake (1968) or Deer, Howie, and Zussman (1963). Tie lines connect analyses of coexisting hornblende and glaucophane of Himmelberg and Papike (1969). Concentration centered approximately at a residual value of +0.15 and $x/(x+y)=0.25$.

or "edenitic hornblende" (labelled "E" on Fig. 6) by Deer, Howie, and Zussman (1963) and Leake (1968) fall very far from the edenite point and are most typically hornblendes with a large amount of Na substitution in $M(4)$, thus possessing a glaucophane-like or richterite-like substitu-

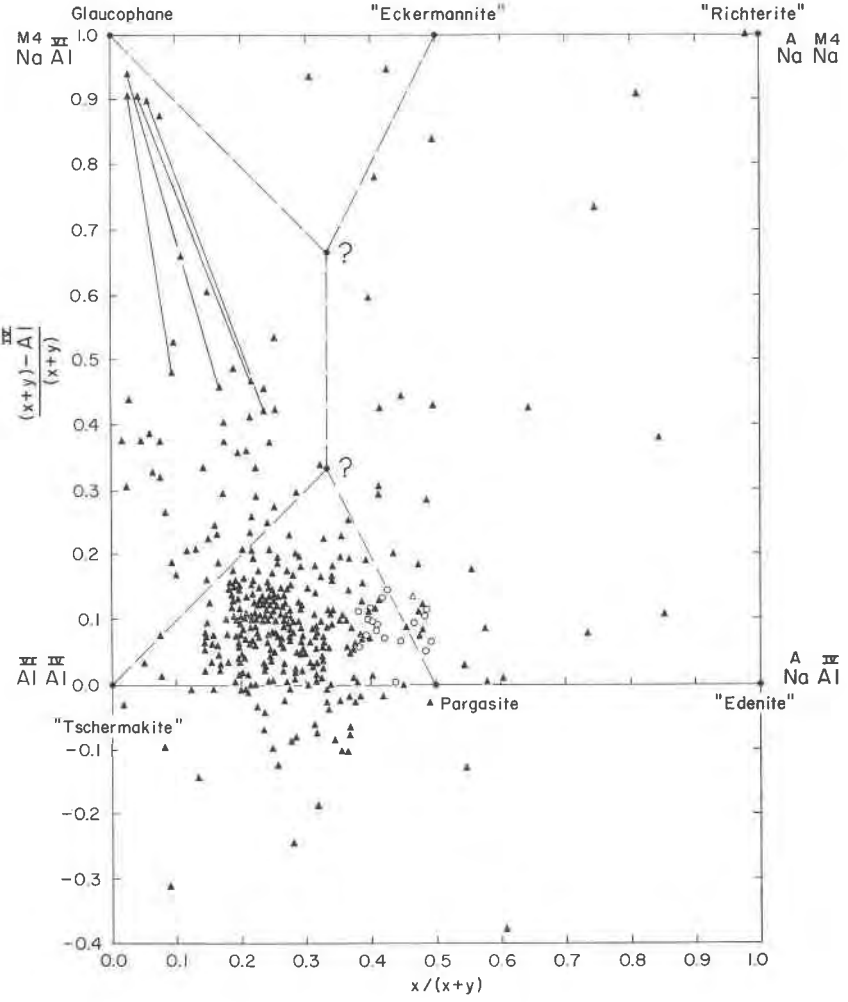

FIG. 7. Projection of the amphibole composition polyhedron from the tremolite apex onto the glaucophane-tschermakite-edenite-richterite plane showing projected composition of 349 clinoamphiboles (see Fig. 6 and text). The apices labelled ? are the ideal end members labelled ? in figures of Whittaker (1968) and in Table 3.

tion. Analyses with this type of substitution, when plotted in the standard manner with Na+K versus Si (Leake, 1968, Fig. 11) give the impression of having more *A*-site sodium than is actually indicated by examination of individual analyses. Even analyses with a major pargasite substitution, supposedly the most important substitution in common

hornblende (Deer, Howie, and Zussman, 1963, p. 272), are fairly scarce. Exceptions to this are the numerous analyses of hastingsite (the $Fe^{2+}Fe^{3+}$ analogue of pargasite) from both quartz- and feldspathoid-bearing intrusives in Rhodesia (Henderson, 1968) with $x/(x+y)$ from 0.380 to 0.490 (special symbol, Figs. 6, 7). All of these amphiboles are quite potassic, with a ratio of K/(K+Na) of around 0.33, and very rich in Fe, which could be related to their very high A occupancies and their consistent compositional difference from the main cluster.[1] By contrast there is a tremendous concentration of analyses near $x/(x+y)=0.25$ in very close agreement with the concentration of anthophyllite analyses in Figure 5. This emphasizes the similarity of the anthophyllite and hornblende groups in respects other than the occupancy of the $M(4)$ sites and suggests a similar crystal-chemical control between A occupancy and tetrahedral Al in both mineral groups.

The main concentration in Figure 6 is centered at a residual value of about +0.15. The most probable explanation for this is that many individual analyses have about 0.15 Na ions in the $M4$ site. This substitution was well demonstrated for a number of Australian hornblende analyses by Binns (1965).

Figure 7 shows precisely the *directions* in which calcic amphiboles depart from ideal tremolite, but not the *amount* of the departure. By selecting only the 221 analyses close to the tschermakite-edenite line with residuals between +0.20 and −0.20, thus eliminating all analyses with important glaucophane- or richterite-like substitutions, the *amount* of departure from ideal tremolite or actinolite can be shown (Fig. 8) and compared to the anthophyllite-gedrite series (Fig. 4). The similarity between hornblendes and anthophyllites is striking, and the scarcity of edenite, pargasite, and tschermakite compositions is again emphasized. Of the analyses close to pargasite, other than those given by Henderson (1968), most are inferior (marked by brackets in Fig. 8) according to the criteria of Leake (1968), and none are superior. Few superior analyses from Leake show tetrahedral Al greater than 2.0. The three analyses closest to tschermakite (Leake, numbers 484, 575, 868) are indicated by Leake as superior, but all three are very high in octahedral ferric iron rather than aluminum, and their low calculated A-site occupancies could be a result of oxidation by weathering or an error in the ferric determination.

Although showing much scatter, the crudely linear grouping of the analyses in Figure 8 is striking and suggests, by visual estimate, a solid

[1] Note added in proof: Analyses of granulite facies hornblendes of Leelanandam (1970) show a high ratio $x/(x+y)$ and high Fe^{3+} content like the hastingsites from Rhodesia, but have a highly variable K/K+Na, suggesting that K cannot be the explanation.

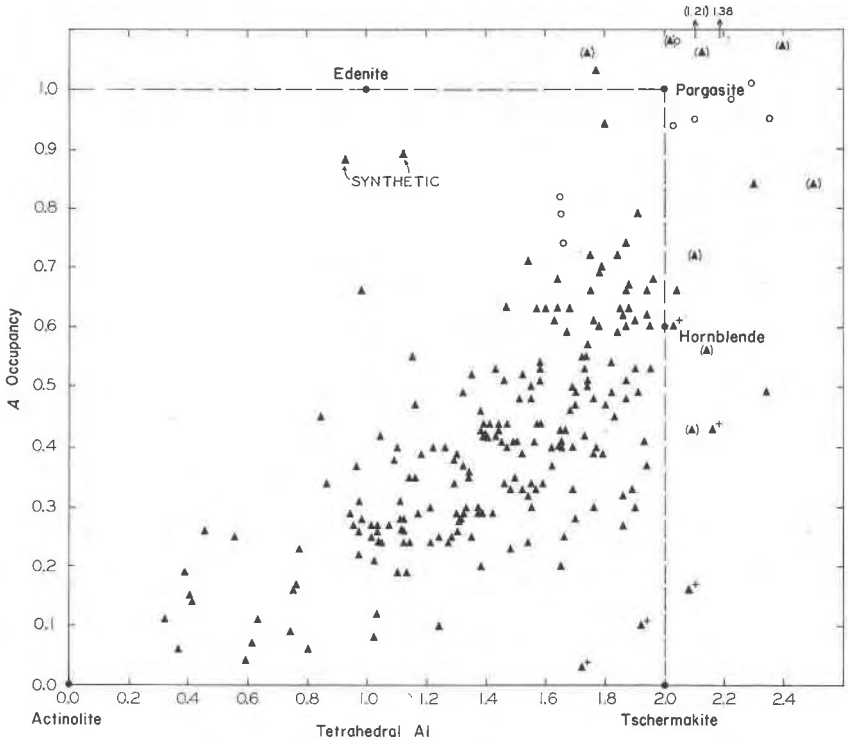

FIG. 8. Plot of A-site occupancy against tetrahedral Al for 221 clinoamphibole analyses close to the tschermakite-edenite line on Figure 6 with residual values between +0.2 and −0.2. These analyses lack important glaucophane- or richterite-like substitutions. In areas near pargasite and tschermakite quality of analyses according to Leake (1968) are indicated thus: cross, superior analysis; brackets, inferior analysis; unmarked, intermediate quality analysis.

solution series essentially between actinolite and a hornblende with the ideal formula shown in Table 4, that compares closely with the ideal gedrite formula discussed above. It is interesting that the 1.4 octahedral Al in the ideal hornblende formula corresponds to the maximum amount of octahedral Al found by Leake (1965) in a survey of highly aluminous hornblendes.

Since the anthophyllite-gedrite and actinolite-hornblende series form two parallel solid solutions, they can be partially represented in a ternary reciprocal system (Fig. 9) in which compositions of coexisting pairs can be shown.[2] Figure 9 shows an interesting fractionation in which the calcic

[2] Note added in proof: A wet analyzed hornblende-anthophyllite pair from the Tanzawa Mountains, Japan reported by Tiba, Hashimoto, and Kato (1970) falls neatly in the blank central part of Figure 9. Hornblende and anthophyllite contain tetrahedral Al of 1.146 and 0.315, and Ca/(Ca+R^{2+}) in $M(4)$ of 0.816 and 0.074 respectively.

TABLE 4. SUGGESTED STRUCTURAL FORMULAE FOR NATURAL GEDRITE AND HORNBLENDE END COMPOSITIONS CHARACTERIZATIONS ACCORDING TO THE IDEAL FORMULA IN TABLE 2

	x	y	$x+y$	Al^{IV}	$(x+y)$-Al^{IV}	$x/(x+y)$
Gedrite	0.5	1.5	2.0	2.0	0.0	0.25
Hornblende	0.6	1.4	2.0	2.0	0.0	0.30

Gedrite $Na_{0.5}(Mg, Fe)_2[(Mg, Fe)_{3.5}(Al, Fe^{3+})_{1.5}](Al_2Si_6)O_{22}(OH)_2$

Hornblende $Na_{0.6}Ca_2[(Mg, Fe)_{3.6}(Al, Fe^{3+})_{1.4}](Al_2Si_6)O_{22}(OH)_2$

amphibole concentrates Na and Al relative to the coexisting anthophyllite. However, in more highly aluminous rocks not containing calcic amphibole, gedrite may contain a higher Na and Al content than any hornblende formed under the same conditions. Note also that the hornblende admits more Mg and Fe^{2+} into $M(4)$ than the anthophyllite admits Ca (and commonly contains primitive cummingtonite exsolution lamellae). Hornblende and anthophyllite are thus directly analogous in this respect to the pyroxenes augite and hypersthene (Hess, 1941). The explanation is clearcut. In hornblende the $M(4)$ and in augite the equivalent $M(2)$ sites are large, but the monoclinic structure is flexible permitting shifts to accommodate the smaller Fe^{2+} and Mg ions (Papike, Ross,

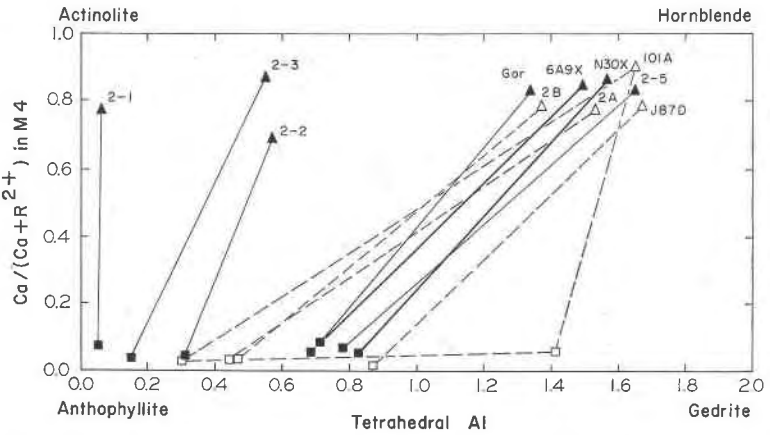

FIG. 9. The actinolite-hornblende-anthophyllite-gedrite ternary reciprocal system showing pairs of coexisting hornblendes and anthophyllites, and one hornblende-anthophyllite-gedrite assemblage (appendix). Hornblendes 2B and 2A represent primary and secondary hornblende respectively from the same thin section. The secondary hornblende is richer in Al and shows a stronger fractionation of tetrahedral Al with coexisting anthophyllite, consistent with a lower temperature of formation.

and Clark, 1969; Clark, Appleman, and Papike, 1969). In anthophyllite the $M(4)$ and in hypersthene the equivalent $M(2)$ sites are small and locked into essentially six coordination, hence they cannot accommodate substantial Ca (Papike and Ross, 1970; Finger, 1970; Warren and Modell, 1930).

Under some conditions miscibility gaps can be expected both in the anthophyllite-gedrite and actinolite-hornblende series (Shido and Miyashiro, 1959; Compton, 1958; Klein, 1969). Indeed, it was the known gap between actinolite and hornblende that made J. B. Thompson, Jr. suggest, in 1968, that we search for the structurally analogous anthophyllite-gedrite gap. The fractionation shown in Figure 9 indicates that, under conditions where both gaps are open, anthophyllite would coexist with hornblende but actinolite would not occur with gedrite. The three-amphibole assemblages anthophyllite-actinolite-hornblende and anthophyllite-gedrite-hornblende would be expected in appropriate bulk compositions under these conditions. The second of these has been well documented by Stout (1971).

Crystallographic Significance of Half Occupancy of the A Site in Gedrite and Hornblende

The data given above strongly indicate ideal gedrite and ideal hornblende formulae with A-site occupancy at or close to 0.5. This suggests that both the ortho- and clinoamphibole structures may contain two structurally distinct A sites. Thompson (1970) proposed an ideal model amphibole structure with a ratio of O-rotated to S-rotated tetrahedral chains of 3:1, that contains two structurally distinct A sites. The real gedrite and anthophyllite structures as deduced by Papike and Ross (1970) and Finger (1970) contain no S-rotated tetrahedral chains, but two sets of O-rotated chains with different degrees of rotation. One set of chains (A chains) shows a mild violation of the parity rule demonstrated by Thompson. This set of chains is, however, closer to a fully extended arrangement than the more strongly rotated (B) chains, and a slight distortion of the $M(2)$ octahedra permits this structure to fit together. Neither refined structure contains structurally distinct A sites, although both bear a weak similarity to Thompson's model amphibole in space group $P2_1ma$ which does contain two A sites. Available single crystal data on hornblendes (Ross, Papike, and Shaw, 1969) shows that all belong to space group $C2/m$ in which structurally distinct A sites are not possible. Primitive space groups have greater possibilities for two distinct A sites as discussed by Papike and Ross (1970). Lacking concrete evidence for structurally distinct A sites, an investigation should be made on the physical constraints the structure may have on the limits of various substitutions, to attempt to resolve this question.

Compositional Limits of the Anthophyllite-Gedrite Field

The size and shape of the anthophyllite-gedrite field is a function of the pressure, temperature, and activity of H_2O prevailing during metamorphism. It is controlled in detail by the relative stabilities of orthoamphibole and such competing phases as other amphiboles, quartz, plagioclase, garnet, cordierite, chlorite, staurolite, or aluminum silicates. Figure 10 is an attempt to portray the composition field of anthophyllite-gedrite in terms of Fe/Mg ratio and tetrahedral Al content for the metamorphic conditions prevailing in the sillimanite zone, southwestern New Hampshire and adjacent Massachusetts (Robinson and Jaffe, 1969b). Figure 11 shows a large number of anthophyllite-gedrite analyses plotted in the same manner as in Figure 10.

On the extreme low Al edge of the anthophyllite field in the "Amphibole Hill area" (Fig. 10) for *fe*[1] greater than 40, anthophyllite coexists with cummingtonite, the composition field of which is shown directly. The lengths and positions of anthophyllite-cummingtonite tie lines are a function of amphibole crystal chemistry only. However, because of the Na and Ca contents of both minerals (Robinson and Jaffe, 1969b, Fig. 8) the length and orientation of tie lines may be slightly different in plagioclase-saturated bulk compositions than in those poorer in Na and Ca, and could appear differently on Figure 10.

We can infer the composition of a hypothetical anthophyllite that coexists with both cummingtonite and hornblende in the "Amphibole Hill area" and that plots in Figure 10 on the low Al boundary of the anthophyllite field at $fe = 40.5$. Although we do not have an analysis of such an anthophyllite from the sillimanite zone, we do have one from the sillimanite-orthoclase zone (QB27C) with $fe = 36$ consistent with different metamorphic conditions (Robinson, Jaffe, Klein, and Ross, 1969).

Analyses N30X and 6A9X represent the compositions of anthophyllites coexisting with hornblende and plagioclase. In this case the presence of plagioclase is critical to the boundary shown, and in plagioclase-free (*i.e.* ultramafic) rocks the anthophyllite field extends all the way to ideal pure magnesian anthophyllite. In plagioclase-free rocks there is also an extension of the cummingtonite field toward lower Fe contents (Robinson and Jaffe, 1969b, analysis NO1B; Kisch, 1969), and presumably there exists a field of coexisting Mg-rich anthophyllite and Mg-rich cummingtonite, the boundaries of which are shown by the short dashed lines in Figure 10. The more coarsely shaded area near analysis QB27C represents the extended field of anthophyllite coexisting with plagioclase under conditions of the sillimanite-orthoclase zone.

On the high Al, high Mg edge, the anthophyllite-gedrite field is limited

[1] $fe = 100(FeO+MnO)/(FeO+MnO+MgO)$.

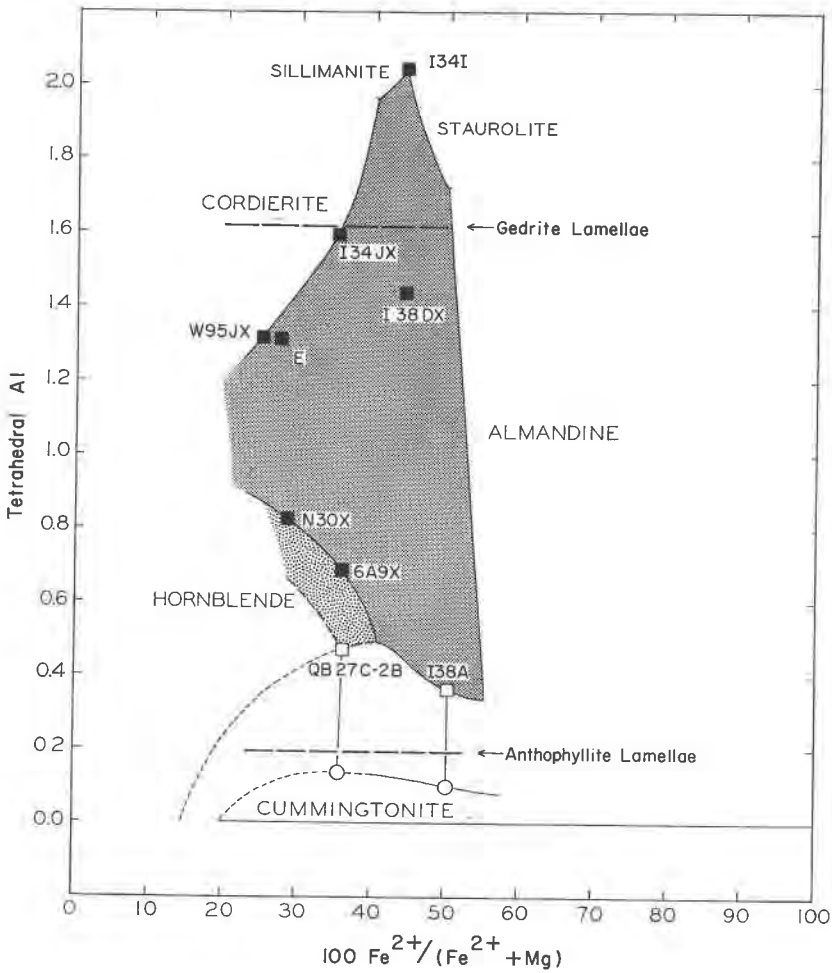

FIG. 10. Composition field of anthophyllite-gedrite coexisting with plagioclase in terms of Fe^{2+}/Mg ratio and tetrahedral Al for primary metamorphic conditions in the sillimanite zone ("Amphibole Hill Area"), southwestern New Hampshire and adjacent Massachusetts. Mn^{2+} is included in Fe^{2+}. For details of assemblages see Robinson and Jaffe (1969b, Table 1). Boundaries of the field are defined by the coexistance of anthophyllite with various other phases. Closed squares, wet analyses of anthophyllites; open squares, probe analyses of anthophyllites; open circles, probe analyses of cummingtonites. Tetrahedral Al contents for secondary anthophyllite and gedrite exsolution lamellae are inferred from Figure 14.

by its coexistence with cordierite. It is probable that the presence or absence of plagioclase has little effect on the position of this boundary, but it is possible that undersaturation with respect to quartz could permit

a slightly higher tetrahedral Al than in the presence of quartz. Because specimen I34JX contains both quartz and plagioclase, whereas W95JX contains neither, this effect is probably very slight. The sharp increase in tetrahedral Al with increasing *fe* along the cordierite-saturated edge of

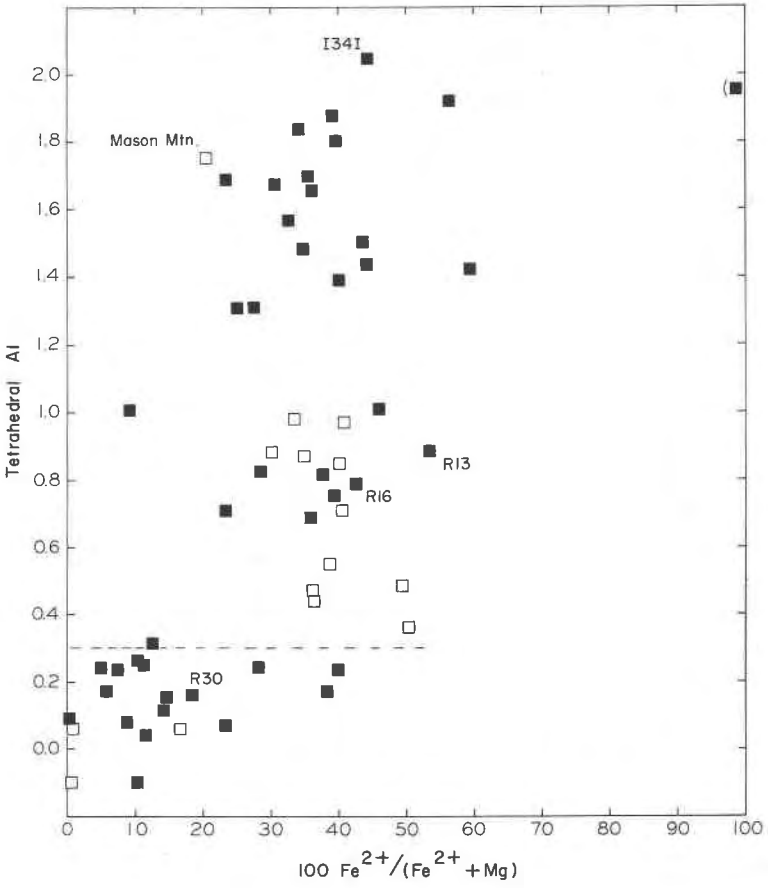

FIG. 11. Compositions of analyzed anthophyllites (see appendix) plotted in terms of Fe^{2+}/Mg ratio and tetrahedral Al. Mn^{2+} is included in Fe^{2+}. Samples from Mason Mtn. and number I34I are gedrites 001 and 002 respectively for which the structure has been determined by Papike and Ross (1970). Anthophyllite R30 is from Rabbit (1948, number 30) for which the structure has been determined by Finger (1970). R16 and R13 are from Rabbit (numbers 16 and 13), the light and dark anthophyllites coexisting with cordierite analyzed by Eskola (1914). Bracketed analysis is from Seki and Yamasaki (1957) for which they made a correction for 6% chlorite impurity. Above the dashed line at a value of 0.3 tetrahedral Al, the only analyses plotted are those that survived the screening process described in the text.

the anthophyllite-gedrite field shows that magnesian cordierite competes far more successfully against gedrite than does more iron-rich cordierite under these metamorphic conditions. Under other, probably lower pressure, metamorphic conditions cordierite is far more successful than here. For example at Orijärvi, Finland (Eskola, 1914) cordierite coexists with anthophyllites that have a tetrahedral Al content of only 0.78 and 0.88 (Fig. 11). There is a possibility that the cordierite-saturated and hornblende+plagioclase-saturated edges of the anthophyllite field intersect in the vicinity of tetrahedral Al = 1.0, $fe = 10$. This leads to speculation that there could be a stable association of quartz, plagioclase, hornblende, and cordierite for extremely magnesian compositions. A rock containing hornblende and cordierite together with anthophyllite and cummingtonite has been described by Goroshnikov and Yur'yev (1965) but the described textural relations are not easily interpreted.

In the extreme Al-rich corner of the anthophyllite-gedrite field gedrite coexists with quartz, kyanite, and sillimanite. It is possible that tetrahedral Al could go higher in a silica-undersaturated rock unless a tetrahedral Al content of 2.0 is a crystal chemical limit as suggested by Papike, Ross, and Clark (1969). The staurolite-saturated edge seems to be a true limit, because staurolite itself is low in silica. The almandine-saturated edge also appears to be very close to a true limit under these conditions. Garnets containing appreciable amounts of components other than almandine and pyrope, in particular spessartine, can coexist with anthophyllites with a lower Fe content than the high Fe limit of the anthophyllite field, and such garnets do in fact occur in specimens I34I, I38DX, and I38A. The ferrogedrite composition given by Seki and Yamasaki (1957) shows that, in the andalusite zone of an andalusite-sillimanite contact aureole, gedrite is far more successful in competing against staurolite and garnet than it is here.

Exsolution Lamellae in Anthophyllites and Gedrites

X-ray single crystal studies (Ross, Papike, and Shaw, 1969) were made on six wet analyzed anthophyllites and gedrites, and one electron probe analyzed anthophyllite (Table 5). The five specimens lowest in tetrahedral Al give doubled reflections showing they are actually intergrowths of two orthorhombic amphiboles, both having space group *Pnma*, and differing in their *b* crystallographic dimensions. The difference between the *b* dimensions and comparison with the two homogeneous gedrites indicates that the two sets of lamellae are gedrite and anthophyllite.

After discovery of exsolution in X-ray photographs of five specimens, careful optical examination revealed pervasive fine (010) lamellae in the

TABLE 5. TETRAHEDRAL Al CONTENT, SINGLE CRYSTAL X-RAY DATA, MICROSCOPE AND HAND SPECIMEN OBSERVATIONS OF ANALYZED ANTHOPHYLLITES

	Al^{IV}	% Gedrite[b]	Gedrite *b* in Å	Anth. *b* in Å	Visible (010) Lamellae	Schiller Effect in Hand Specimen
I34I	2.05	100	17.839[c]		None	None
I34JX	1.60	100	17.81		Trace	None
I38DX	1.44	80	17.87	18.11	Pervasive	None
W95JX	1.32	80	17.76	17.98	Pervasive	Minor
N30X	.82	50	17.84	18.04	Trace	Strong
6A9X	.68	30	17.88	18.05	None	Strong
QB27C-2B	.47[a]	20	17.81	18.00	None	Moderate

[a] Electron probe analysis.

[b] Estimated very approximately from relative intensities of the gedrite and anthophyllite reflections in X-ray Buerger precession photographs (Ross, Papike, and Shaw, 1969) of one crystal from each sample.

[c] Dimensions measured on X-ray single crystal precession photographs, accurate to ±0.02Å, except I34I obtained by least-squares refinement of x-ray diffraction powder data.

two most aluminous of these (W95JX and I38DX, Table 5). Lamellae were also observed at a few points in specimens I34JX and N30X. The lamellae are most clearly visible in specimen I38DX, a photomicrograph of which is given in Figure 12. The lamellae are estimated to be 0.2 microns and 0.8 microns thick. The photomicrograph was taken with b ($= Y$) oriented parallel to the lower polarizer and with the image thrown slightly out of focus by racking the microscope stage slightly down away from the lens system. This apparently had the effect of making the Becke lines move *out* of the thin lamellae causing the thin lamellae to appear dark and the thick lamellae to appear light. From this we conclude that the index of refraction (β) is lower in the thin lamellae than in the thick lamellae. Comparison of indices of refraction of two sets of gedrite and anthophyllite that are optically homogeneous or nearly so, and have a similar Fe content, yields the following information:

	FeO/(FeO+MgO)	Fe per 23(O)	β
Gedrite I34JX	.35	2.159	1.661
Anthophyllite 6A9X	.36	2.259	1.656
Gedrite 101A (Stout 1970c)	.44	2.70	1.662
Anthophyllite 101A (Stout 1970c)	.40	2.62	1.650

Thus for a given Fe content a gedrite would have a higher index than an anthophyllite, and we conclude that the thin lamellae (0.2 μm thick) in specimen I38DX are anthophyllite and the thick lamellae (0.8 μm thick) are gedrite. The relative widths of the lamellae are in agreement with the

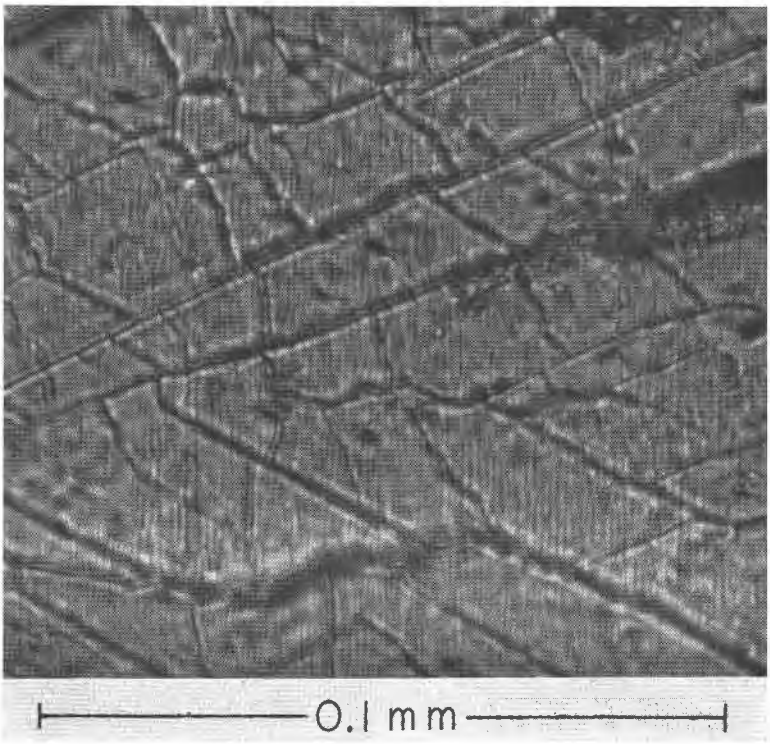

FIG. 12. Photomicrograph in plane polarized light of a thin section cut roughly normal to the c axis of gedrite I38DX showing exsolution lamellae parallel to (010) that bisect the obtuse angle between {110} cleavages. Pairs consisting of one dark anthophyllite lamella and one light gedrite lamella (see text) are estimated to be 1 μm thick, and the individual dark and light lamellae are about 0.2 and 0.8 μm thick respectively. Note branching of lamellae and variable thickness.

relative abundance estimated in the single crystal photograph and demonstrate that the lamellae detected by the two methods are the same.

Anthophyllites N30X, 6A9X, and QB27C-2B show little or no evidence in thin section of the exsolution demonstrated by the X-ray photographs. However, in hand specimens they show a strong schiller effect with variable blue, green, and yellow colors, in some cases with blue centers and yellow edges. Investigations under the electron microscope of plagioclases showing similar colors (Fleet and Ribbe, 1965; Laves, Nissen, and Bollmann, 1965; Bolton, Bursill, McLaren, and Turner, 1966; Nissen, Eggmann, and Laves, 1967) have shown that these contain alternate plagioclase lamellae of different diffraction contrast. These lamellae, when combined, give a repeat unit in the range 0.14 to

0.22 μm which is appropriate for the diffraction of light according to the Bragg equation, provided the repeat unit d is multiplied by the index of refraction. The observed schiller in anthophyllites suggests a diffraction grating set up by exsolved lamellae of statistical periodicity. For the observed schiller colors with wavelengths from 0.47 μm (blue) to 0.58 μm (yellow), assuming an angle θ of 80° and an index of refraction 1.66, the Bragg equation indicates the anthophyllites with schiller have a repeat unit in the range 0.14 to 0.18 μm, as compared to 1.0 μm for the specimens with lamellae visible under the light microscope. The lamellae in the schiller anthophyllites are apparently just below the resolving power of the light microscope.

The only previously reported schiller in orthoamphibole that we are aware of was described by Boggild (1905, 1924). The 1924 paper, his classic examination of colors in feldspars, summarizes briefly in English his earlier findings published in Danish concerning a specimen from Avisisarfik, west Greenland that he studied with a reflection goniometer: "This mineral possesses a luster of a fine blue or sometimes yellowish or reddish color, and the substance is perfectly homogeneous under the microscope. The lamellae are oriented exactly to the face (010) . . . ". Recalculation of the partial chemical analysis (Boggild, 1905, p. 400) to 23(O) gives:

$$Na_{0.31}(Na_{0.12}Ca_{0.13}Fe^{2+}_{1.85}Mg_{4.10}Al_{0.80})(Si_{7.02}Al_{0.98})O_{22}(OH)_2,$$

a bulk composition squarely in the middle of the field of exsolved orthoamphiboles and nearly identical to a specimen I34B (Robinson and Jaffe, 1969b) in which we observed schiller in the field for the very first time. The Greenland specimen was originally collected in 1810 by K. L. Giesecke who called it "labradoriserende Hornblende."

It is interesting that among the five specimens that show exsolution in the X-ray single crystal photographs, only the two with the most aluminous bulk composition consistently show exsolution features coarse enough to be observed under the microscope. Possibly the exsolution process, which must involve ordering of Al ions in the structure, is facilitated by a high content of Al relative to Si.

The Anthophyllite—Gedrite Solvus

The tetrahedral Al content of the exsolution lamellae cannot be determined directly from the measured b dimension because this dimension is strongly dependent on variable content of Fe as well as Ca, Mn, and perhaps Na [in $M(4)$]. The b dimensions for the various unmixed pairs and homogeneous anthophyllites and gedrites are plotted in Figure 13 against the total Fe per 23(O) for the bulk sample. The unmixed phase

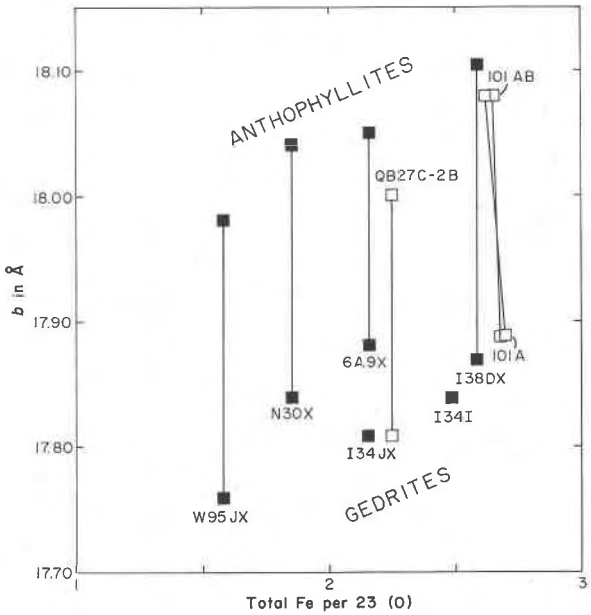

FIG. 13. *b* dimensions from single crystal X-ray photographs of anthophyllites and gedrites plotted against total Fe per 23(O). Closed squares, wet analyses; open squares, probe analyses. Vertical tie lines connect *b* dimensions of the two members of a microscopic or submicroscopic intergrowth for which only the bulk Fe content is known. Assemblages 101A and 101AB from Stout (1970b, c) contain two coarse coexisting orthoamphiboles in which the compositions of each can be determined separately. These four analyses suggest that fractionation of Fe between coexisting anthophyllite and gedrite is probably slight and that the vertical tie lines applied to the other specimens are reasonable.

QB27C-2B, analyzed by electron probe, does not fit well with the other data. This could be due to a difference in composition between probed and X-rayed grains. As might be expected, the *b* dimensions of the two homogeneous gedrites are slightly smaller than the *b* dimensions of gedrite with anthophyllite lamellae of similar bulk Fe content.

The fractionation of Fe and other ions between the anthophyllite and gedrite lamellae is, of course, unknown. However, some indication can be gained from probe analyses of two coarse coexisting orthorhomobic amphiboles from southern Norway reported by Stout (1969, 1970b, 1970c). Total Fe contents based on probe analyses and *b* dimensions from single crystal photographs of these (Stout, 1970c) are also shown in Figure 13. Stout has shown there is essentially no fractionation in total Fe between the two coexisting orthorhombic amphiboles although they differ in their Fe/Mg ratios because Mg in the anthophyllite is replaced

by octahedral Al in the gedrite. The site occupancies determined by Papike and Ross (1970) for gedrite I34I may explain this relationship. In I34I the $M(2)$ site is occupied essentially by Mg and Al with only minor Fe, which may be ferric. The $M(1)$, $M(3)$, and $M(4)$ sites are occupied by Fe and Mg with a strong preference of the large Fe^{2+} ion for the $M(4)$ site. Comparison of Papike and Ross' occupancies in I34I with Stout's coexisting pair suggests the following scheme for exsolution. During exsolution there is a tendency for ordering in the $M(2)$ sites, with Mg concentrating in anthophyllite sites and Al (and probably Fe^{3+}) concentrating in gedrite sites. This is coupled with a concentration of Na in gedrite A sites and concentration of Al in gedrite tetrahedral sites. During this process, at least initially, there may be little or no tendency for Fe/Mg fractionation between $M(4)$ in gedrite and $M(4)$ in anthophyllite, $M(3)$ in gedrite and $M(3)$ in anthophyllite, or $M(1)$ in gedrite and $M(1)$ in anthophyllite, although fractionation between non-equivalent sites both within and between phases could be strong. In this sense the $M(1\text{-}3\text{-}4)$ sites could be conceived of as a relatively inert matrix within which the strong fractionation in $M(2)$, A, and tetrahedral sites, leading to exsolution, took place. Eventually, as the two orthoamphiboles became more different compositionally and structurally, fractionation between equivalent $M(1\text{-}3\text{-}4)$ sites would probably occur. Stout's analyses do suggest a tendency for Ca to concentrate in gedrite and this might help to account for the large b dimensions of gedrites N30X and 6A9X, which show the highest bulk Ca content.

The content of Fe^{3+} inferred by us for gedrite 101A (Table 3) might also have some effect on the b dimension. On crystal-chemical grounds it would be expected that Fe^{3+} would substitute for Al in the $M(2)$ positions, and this would increase the b dimension. It can also be argued that Fe^{3+} (like Al) would concentrate in gedrite rather than anthophyllite, thus influencing one more than the other. Comparisons of equivalent aluminous and ferric clinoamphiboles (Colville, Ernst, and Gilbert, 1966, p. 1746) indicate the ferric substitution has a smaller effect than would be predicted from relative ionic radii. This is consistent with the anticipated higher percentage of covalent bonding between Fe^{3+}-O, electronegativity difference = 1.6, as contrasted with Al-O, electronegativity difference = 2.0 (electronegativity values from Pauling, 1960). Until we have much more information on the compositions of coexisting orthorhombic amphibole pairs, the simplified plot of total Fe against the b dimension is probably best.

Because of the error of $\pm .02$ Å assigned to measurements of the b dimension, variations in the *difference* between b dimensions of pairs in Figure 13 may not be significant. Two out of the five pairs (W95JX,

I38DX) have a larger *difference* in *b* dimension between anthophyllite and gedrite. These are precisely the ones with the pervasive visible lamellae and the highest bulk Al, supporting the previous suggestion that high bulk Al may promote exsolution. The possible effect of Ca on the *b* dimension of gedrites N30X and 6A9X (see above) should, however, be kept in mind. It is important to note also that the Fe content itself does not seem to have an influence on the *difference* in *b* dimension between members of pairs. This suggests that Fe content has little or no influence on the width of the anthophyllite-gedrite miscibility gap in the composition range of the specimens studied.

A crude way to estimate the tetrahedral Al content of the lamellae is to plot the percent of gedrite lamellae visually estimated from the intensities

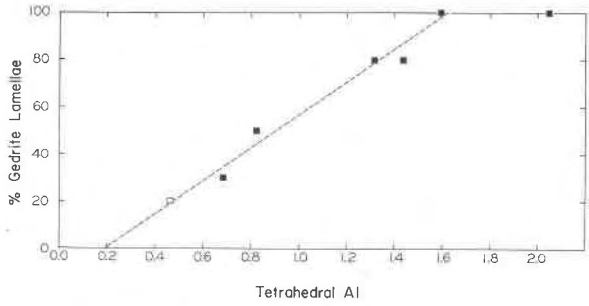

FIG. 14. Percent of gedrite exsolution lamellae as estimated from the intensities of spots in X-ray single crystal photographs plotted against bulk tetrahedral Al for seven analyzed anthophyllites from southwestern New Hampshire and adjacent Massachusetts.

of spots on X-ray photographs (Table 5) against the bulk tetrahedral Al (Fig. 14), assuming that all specimens underwent exsolution under the same conditions. It should be emphasized that the estimates of percentages from X-ray photographs are approximate, with an error of perhaps ± 10 percent, and were made on single grains that may or may not be representative of the analyzed sample. However, the estimates were made with no knowledge of the tetrahedral Al content of the specimens nor anticipation of their use in Figure 14. The assumption of uniform conditions is particularly reasonable in the cases of specimens I34I, I34JX, I38DX, W95JX, and 6A9X which were all collected within 3,000 feet of each other. A linear regression of the data (dashed line Fig. 14) indicates a tetrahedral Al content of about 0.2 atoms per formula unit for the anthophyllite lamellae (0 percent gedrite) and about 1.6 for the gedrite lamellae (100 percent gedrite). Comparison of these suggested lamellae compositions (Fig. 10) with the boundaries of the anthophyllite

field under conditions of primary crystallization, shows that the lamellae compositions fall outside the primary field in many areas. This serves to emphasize that the exsolution process took place in the solid state without chemical exchange with the surrounding rock and under different *P-T* conditions than those of primary crystallization. This could have occurred a long time, perhaps as much as 100 million years, after primary metamorphic crystallization.

The coexisting coarse orthorhombic amphiboles reported by Stout (1969, 1970c) from Telemark, Norway, had a *primary crystallization* under different conditions, possibly lower temperature, than the *primary crystallization* of the specimens from southwestern New Hampshire and Massachusetts. Two pairs of probe analyses of apparently homogeneous amphiboles from one of Stout's hand specimens show that the anthophyllites have 0.30 and 0.34 tetrahedral Al and the gedrites 1.33 and 1.46 tetrahedral Al on the basis of 23(O), or 0.29, 0.34, 1.36, and 1.50 tetrahedral Al respectively, as calculated by Stout (1970c) on the basis of 15 cations exclusive of Na per formula unit. The tetrahedral Al con-

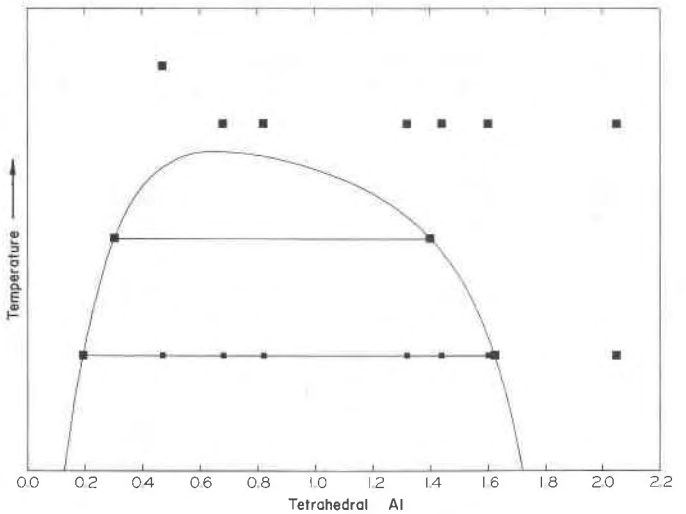

FIG. 15. Speculative temperature-composition diagram for the anthophyllite-gedrite series. Top group of squares represents primary formation of anthophyllites and gedrites from southwestern New Hampshire and Massachusetts. One specimen is shown at higher temperature because it occurs in the sillimanite-orthoclase zone rather than the sillimanite zone. Middle set of squares represents primary formation of coarse coexisting anthophyllite and gedrite in southern Norway reported by Stout (1969, 1970). Bottom set of squares represents secondary exsolution in southwestern New Hampshire and Massachusetts. Small squares show bulk compositions within the solvus that have become two-phase mixtures.

tents of about 0.3 for anthophyllite and about 1.4 for gedrite as compared to 0.2 for anthophyllite lamellae and 1.6 for gedrite lamellae in the New England rocks, might suggest that the *primary crystallization* in the Norwegian rocks took place at a higher temperature than the *exsolution temperature* of the New England specimens. According to Stout (1970c) the Norwegian specimens did not undergo the fine-scale exsolution found in the New England specimens. By combining Stout's data with our own, a highly speculative temperature-composition diagram for the anthophyllite-gedrite series can be drawn (Fig. 15). The asymmetry shown for the solvus is far from definite because of the uncertainties in the calculation of tetrahedral Al content.

Quantitative information on the relative conditions of metamorphism of the Norwegian and New England specimens is lacking. Sillimanite is the Al_2SiO_5 polymorph in the Norwegian area and certain aluminous gedrite rocks contain the assemblage gedrite-cordierite-garnet. In southwestern New Hampshire gedrite rocks of similar compositions contain the assemblages gedrite-cordierite-sillimanite-kyanite and gedrite-staurolite-sillimanite-kyanite. The calculated P-T grid for such compositions given by Robinson and Jaffe (1969b, see also Korikovsky and Teleshova, 1970) shows that the facies types of the two areas are distinguished both by the kyanite=sillimanite equilibrium and by other reactions with comparable positive slopes, with the facies type of the Norwegian rocks on the high T- low P side. Because the anthophyllite-gedrite series does not have a negative volume of mixing, a negative P-T slope for the critical curve is ruled out, and there are two possible relationships between the critical curve, and the kyanite=sillimanite and other reactions that distinguish the two facies types. The critical curve may have a very low positive slope (pressure sensitive) relative to the reactions, in which case the Norwegian rocks would have formed at

FIG. 16. Effect of the introduction of a primary anthophyllite-gedrite solvus on metamorphic facies types similar to those determined for southwestern New Hampshire, shown on a quartz-plagioclase projection.

A. Determined primary phase relations for the "Amphibole Hill Area," above the crest of the solvus.

B. Conditions just below crest of solvus.

C. Conditions with still wider miscibility gap, similar in lower part to relations determined by Stout (1970b) in southern Norway.

The field for the hornblende-cordierite association in all three diagrams is highly speculative.

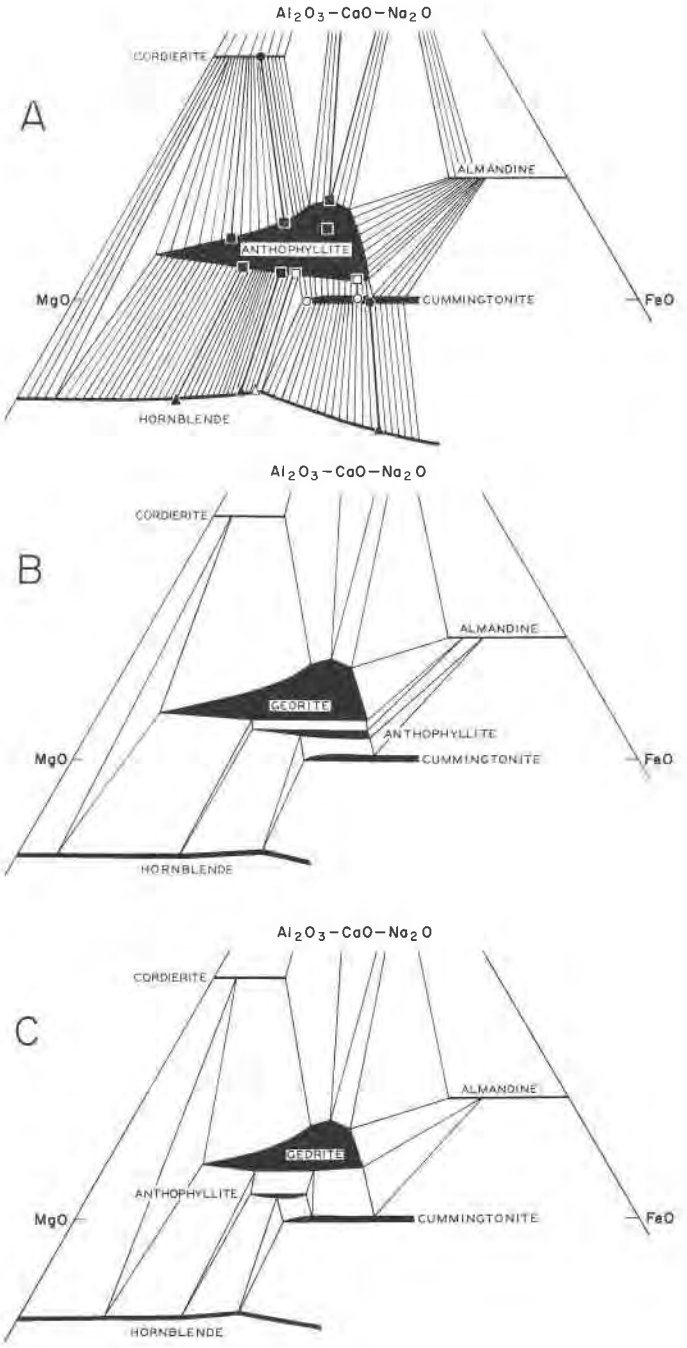
A
$Al_2O_3-CaO-Na_2O$
CORDIERITE
ALMANDINE
ANTHOPHYLLITE
MgO
CUMMINGTONITE
FeO
HORNBLENDE
B
$Al_2O_3-CaO-Na_2O$
CORDIERITE
ALMANDINE
GEDRITE
ANTHOPHYLLITE
MgO
CUMMINGTONITE
FeO
HORNBLENDE
C
$Al_2O_3-CaO-Na_2O$
CORDIERITE
ALMANDINE
GEDRITE
ANTHOPHYLLITE
MgO
CUMMINGTONITE
FeO
HORNBLENDE

higher temperature and higher pressure than the New England rocks. In this case the critical curve would pass at a higher pressure than the alumino-silicate triple point, and most orthoamphiboles in the andalusite zone would be "hypersolvus." Alternatively the critical curve may have a high positive slope (temperature sensitive) relative to the reactions, in which case the Norwegian rocks would have formed at lower pressure and lower temperature than the New England rocks. In this case the

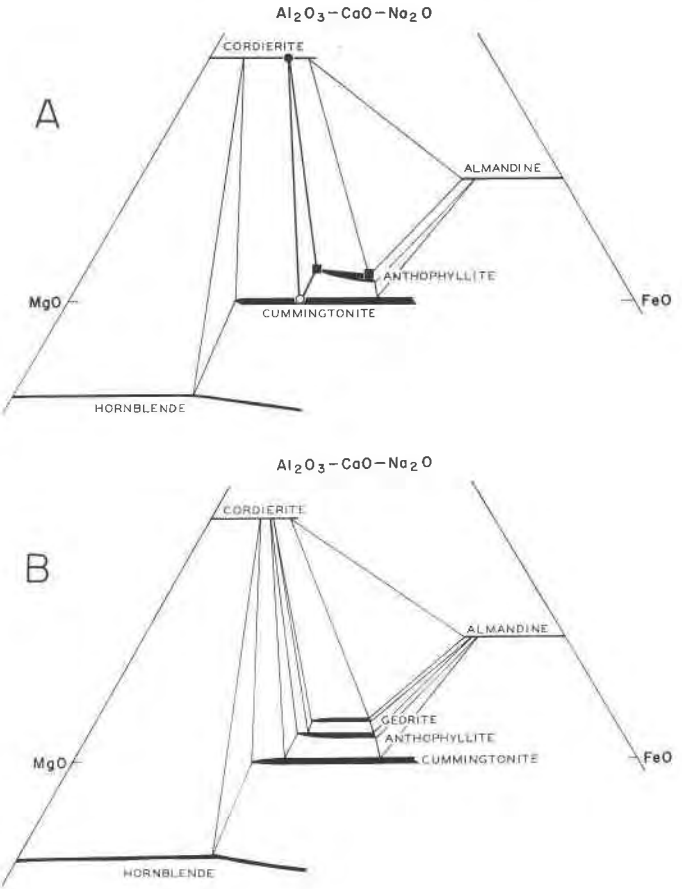

FIG. 17. Effect of the introduction of a primary anthophyllite-gedrite solvus on metamorphic facies types similar to those determined for Träskböle, Orijärvi, by Eskola (1914).

A. Primary phase relations at Träskböle based on data reported by Eskola. Solid figures, wet analyses, open circle-composition of cummingtonite based on optical data and partial analysis.

B. Similar to A. with primary anthophyllite-gedrite solvus.

critical curve would pass at a higher temperature than the aluminosilicate triple point and many orthoamphiboles in the andalusite zone would be "subsolvus." The fact that the structurally analogous subsolvus actinolite-hornblende pair occurs in the classic andalusite-sillimanite type metamorphism of the Abukuma Plateau (Shido and Miyashiro, 1959; Ernst, 1968, p. 69) causes us to lean strongly toward the second alternative and helps to justify our use of temperature on Figure 15.

Metamorphic Facies Types of Anthophyllite—Gedrite Assemblages

Figure 16A represents the determined topological facies relations for the Orange area on a quartz-plagioclase projection (Robinson and Jaffe, 1969b, p. 262–264). Figures 16B and 16C show the same projection and essentially the same topological facies relations except that a primary anthophyllite-gedrite miscibility gap has appeared (16B) and broadened (16C). In portraying the miscibility gap it has been assumed on the basis of data given above, that the Fe/Mg ratio has no influence on the breadth of the gap. Although the upper part is quite different the lower part of Figure 16C is, with certain exceptions, a simplified version of the topological relations suggested by Stout (1970a) for his south Norwegian rocks. Note that there are *three different three-amphibole* fields. Figure 17A represents the facies relations deduced for the Orijärvi district, Finland, on the basis of data of Eskola (1914) (see Robinson and Jaffe, 1969b, Fig. 13D). Under these metamorphic conditions cordierite coexists with anthophyllites with very low tetrahedral Al contents of .78 and .88. Under such circumstances the opening of a miscibility gap could result in the relations shown in Figure 17B. These few examples of metamorphic facies types from a multitude of possibilities illustrate the potential for future chemical petrologic research in anthophyllite-gedrite-bearing rocks.

Acknowledgments

Field, optical, and analytical work and computations at the University of Massachusetts were supported by NSF Research Grants GA-467 (to Jaffe and Robinson), and GA-390 (to Robinson). X-ray studies were done at the U.S. Geological Survey. Farrukh Ahmad and David J. Hall assisted with computations of analyses, Richard Brown assisted with drafting, and several versions of the manuscript were typed by Mrs. Susan Hall and Mrs. Leita Broekhuizen. Mr. Zanis Stuberovskis translated the reference by Korikovsky and Teleshova. James H. Stout, J. J. Papike, and J. B. Thompson, Jr. provided access to their data. Advice was given by Larry W. Finger, Hans-U. Nissen and Stearns A. Morse. The manuscript was reviewed with many beneficial suggestions by Cornelis Klein, Jr., J. J. Papike, James H. Stout, W. Gary Ernst, Stephen Huebner, and Leo M. Hall. To each of these persons and institutions we express our grateful acknowledgment.

References

Binns, R. A. (1965) The mineralogy of metamorphosed basic rocks from the Willyama Complex, Broken Hill district, New South Wales, Part I: Hornblendes. *Mineral. Mag.* **35,** 306–326.

——— (1967) Barroisite-bearing eclogite from Naustdal, Sogn og Fjordane, Norway. *J. Petrology* **8,** 349–371.

Boggild, O. B. (1905) Mineralogia Groenlandica. *Medd. Gronland* **32,** p. 400.

——— (1924) On the labradorization of the feldspars. *K. Danske Videnskab. Selskab, Mat.-Fys. Medd.* **6,** 1–79.

Bolton, H. C., L. A. Bursill, A. C. McLaren, and R. G. Turner (1966) On the origin of the colour of labradorite. *Phys. Status Solidi* **18,** 221–230.

Clark, J. R., D. E. Appleman, and J. J. Papike (1969) Crystal-chemical characterization of clinopyroxenes based on eight new structure refinements. *Mineral. Soc. Amer. Spec. Pap.* **2,** 31–50.

Colville, P. A., W. G. Ernst, and M. C. Gilbert (1966) Relations between cell parameters and chemical compositions of monoclinic amphiboles. *Amer. Mineral.* **51,** 1727–1754.

Compton, R. R. (1958) Significance of amphibole paragenesis in the Bidwell Bar region, California. *Amer. Mineral.* **43,** 890–907.

Deer, W. A., R. A. Howie, and Jack Zussman (1963) *Rock-forming Minerals, Vol. 2, Chain Silicates.* John Wiley and Sons, New York, 379 p.

Dodge, F. C. W., J. J. Papike, and R. E. Mays (1968) Hornblendes from granitic rocks of the Central Sierra Nevada batholith, California. *J. Petrology* **9,** 378–410.

Ernst, W. G. (1968) *Amphiboles.* Springer-Verlag, New York, 125 p.

Eskola, Pentti (1914) On the petrology of the Orijarvi region in southwestern Finland. *Bull. Comm. Geol. Finlande* **40.**

Finger, L. W. (1970) Refinement of the crystal structure of an anthophyllite. *Carnegie Inst. Wash. Year Book* **68,** 283–288.

Fleet, S. G., and P. H. Ribbe (1965) An electron microscope study of peristerite plagioclases. *Mineral. Mag.* **35,** 165–176.

Goroshnikov, V. I., and L. D. Yur'yev (1965) Cordierite-polyamphibole and anthophyllite-cordierite rocks of the North Krivoy Rog District. *Dokl. Akad. Nauk SSSR* **163,** 720–723 [Transl. *Acad. Sci. U.S.S.R. Doklady, Earth Sci. Sec.* **163,** 140–143 (1967)].

Henderson, C. M. B. (1968) Chemistry of hastingsitic amphiboles from the Marangudzi igneous complex, Southern Rhodesia. *Int. Mineral. Assoc. Pap. Proc., 5th Gen. Meet.,* Cambridge, 1966, p. 291–304.

Hess, H. H. (1941) Pyroxenes of common mafic magmas: Part 2. *Amer. Mineral.* **26,** 573–594.

Himmelberg, G. R., and J. J. Papike (1969) Coexisting amphiboles from blueschist facies metamorphic rocks. *J. Petrology* **10,** 102–114.

Kisch, H. J. (1969) Magnesiocummingtonite-$P2_1/m$: a Ca- and Mn-poor clinoamphibole from New South Wales. *Contrib. Mineral. Petrology* **21,** 319–331.

Klein, Cornelis, Jr. (1968) Coexisting amphiboles. *J. Petrology* **9,** 281–330.

——— (1969) Two-amphibole assemblages in the system actinolite-hornblende-glaucophane. *Amer. Mineral.* **54,** 212–237.

Korikovsky, S. P., and R. L. Teleshova (1970) [The staurolite in cordierite-sillimanite schists of the Udukansk Series and the upper boundary of the staurolite facies in andalusite-sillimanite complexes] *Dokl. Akad. Nauk SSSR,* **191,** 429–432 [in Russian].

LALL, R. K., AND W. W. MOORHOUSE (1969) Cordierite-gedrite rocks and associated gneisses of Fishtail Lake, Harcourt Township, Ontario. *Can. J. Earth Sci.* **6,** 145–165.

LAVES, FRITZ, H. U-.NISSEN, AND W. BOLLMANN (1965) On schiller and submicroscopical lamellae of labradorite. *Naturwissenschaften* **52,** 427–428.

LEAKE, B. E. (1965) The relationship between tetrahedral aluminum and the maximum possible octahedral aluminum in natural calciferous and subcalciferous amphiboles. *Amer. Mineral.* **50,** 843–851.

——— (1968) A catalog of analyzed calciferous and subcalciferous amphiboles together with their nomenclature and associated minerals. *Geol. Soc. Amer. Spec. Pap.* **98,** 210 p.

LEELANANDAM, C. (1970) Chemical mineralogy of hornblendes and biotites from the charnockitic rocks of Kondapalli, India. *J. Petrology* **11,** 475–505.

MILTON, D. J., AND JUN ITO (1961) Gedrite from Oxford County, Maine. *Amer. Mineral.* **46,** 734–740.

MOORE, P. B. (1969) Joesmithite: A novel amphibole crystal chemistry. *Mineral. Soc. Amer. Spec. Pap.* **2,** 111–115.

NISSEN, H.-U., H. EGGMANN, AND FRITZ LAVES (1967) Schiller and submicroscopic lamellae of labradorite. *Schweiz. Mineral. Petrogr. Mitt.* **47,** 289–302.

PAPIKE, J. J., AND MALCOLM ROSS (1970) Gedrites: Crystal structures and intracrystalline cation distributions. *Amer. Mineral.* **55,** 1945–1972.

———, ———, AND J. R. CLARK (1969) Crystal-chemical characterization of clinoamphiboles based on five new structure refinements. *Mineral. Soc. Amer. Spec. Pap.* **2,** 117–136.

PAULING, LINUS (1960) *The nature of the chemical bond.* Cornell University Press, Ithaca, 64–107.

PHILLIPS, R. (1966) Amphibole compositional space. *Mineral. Mag.* **35,** 945–952.

———, AND W. LAYTON (1964) The calciferous and alkali amphiboles. *Mineral. Mag.* **33,** 1097–1109.

RABBITT, J. C. (1948) A new study of the anthophyllite series. *Amer. Mineral.* **33,** 263–323.

ROBINSON, PETER, AND H. W. JAFFE (1969a) Aluminous enclaves in gedrite-cordierite gneiss from southwestern New Hampshire. *Amer. J. Sci.* **267,** 389–421.

———, AND ——— (1969b) Chemographic exploration of amphibole assemblages from central Massachusetts and southwestern New Hampshire. *Mineral. Soc. Amer. Spec. Pap.* **2,** 251–274.

———, ———, CORNELIS KLEIN, JR., AND MALCOLM ROSS (1969) Equilibrium coexistence of three amphiboles. *Contrib. Mineral. Petrology* **22,** 248–258.

ROSS, MALCOLM, J. J. PAPIKE, AND K. W. SHAW (1969) Exsolution textures in amphiboles as indicators of subsolidus thermal histories. *Mineral Soc. Amer. Spec. Pap.* **2,** 275–299.

SEKI, YOTARO, AND MASAO YAMASAKI (1957) Aluminian ferroanthophyllite from the Kitakami mountainland, north-eastern Japan. *Amer. Mineral.* **42,** 506–520.

SHIDO, FUMIKO, AND AKIHO MIYASHIRO (1959) Hornblendes of basic metamorphic rocks. *J. Fac. Sci. Univ. Tokyo, Sec. II* **12,** 85–102.

SMITH, J. V. (1959) Graphical representation of amphibole compositions. *Amer. Mineral.* **44,** 437–440.

STOUT, J. H. (1969) An electron microprobe study of coexisting orthorhombic amphiboles (Abstr.). *Trans. Amer. Geophys. Union* **50,** 359.

——— (1970a) Three-amphibole assemblages and their bearing on the anthophyllite-gedrite miscibility gap (abstr.). *Amer. Mineral.* **55,** 312–313.

——— (1970b) *Geology of the Fyresvatn-Nisser area, Telemark, Norway.* Ph.D. Thesis, Harvard University.

——— (1971) Four coexisting amphiboles from Telemark, Norway. *Amer. Mineral.* **56,** 212–224.

THOMPSON, J. B., JR. (1970) Geometrical possibilities for amphibole structures: model biopyrobiles (Abstract). *Amer. Mineral.* **55,** 292–293.

TIBA, TOKIKO, MITSUO HASHIMOTO, AND AKIRA KATO (1970) An anthophyllite-hornblende pair from Japan. *Lithos* **3,** 335–340.

WARREN, B. E., AND D. I. MODELL (1930) The structure of enstatite $MgSiO_3$. *Z. Kristallogr.* **75,** 1–14.

WHITTAKER, E. J. W. (1968) Classification of the amphiboles. *Proc. Int. Mineral. Assoc. Pap., Proc. 5th Gen. Meet.*, Cambridge, 1966, 232–242.

Manuscript received, September 22, 1970; accepted for publication, December 23, 1970.

Appendix: Sources of Analyses Used for Figures.

FIG. 2. Analyses used for Figure 1. Deer, Howie, and Zussman (1963); anthophyllites 2, 3, 5–11; gedrites 2–10. Rabbitt (1948), 1, 5, 7, 8, 11, 13, 16, 19, 25, 26, 30, 32, 34, 40, 42, 43, 45 (these are in addition to analyses quoted by Deer, Howie, and Zussman). Klein (1968) (in addition to analyses reported above); wet analyses 2-1, 2-2, 2-4; probe analyses 3-1, 3-2, 3-3. Milton and Ito (1961), one wet analysis. Lall and Moorhouse (1969), wet analyses 80, 112. New probe analysis of Mason Mountain, North Carolina (Papike and Ross, 1970, gedrite 001; Deer, Howie and Zussman, gedrite 1) by U.S. Geological Survey (Papike and Ross, personal communication). Goroshnikov and Yur'yev, 1965, Table 2, No. 3. Stout (1969, 1970c), two anthophyllite-gedrite pairs.

FIG. 3. Robinson and Jaffe, 1969b, Table 2, I34I, I34JX, and I34JX with total Fe recalculated as FeO. Deer, Howie, and Zussman (1963), anthophyllites 9, 10; gedrites 5, 8, 9, 10. Rabbitt (1948), 5, 7, 16. Milton and Ito (1961), one analysis. Lall and Moorhouse (1969), 80, 112, and 112 with total Fe recalculated as FeO. Stout (1970c), 101AB and 101AB assuming $X/Al^{IV}=.25$ and Fe^{3+}/Fe total$=.26$.

FIGS. 4 and 5. This paper Table 1. Robinson and Jaffe, 1969b, Table 4, all except 6A9 which shows .09 Ca in *A*. Deer, Howie, and Zussman (1963), anthophyllite 5, gedrites 2, 4, 6. Rabbitt (1948), 1, 19. New probe analysis of Mason Mtn., N.C. The following analyses from published sources were recalculated on basis of 23(O): Deer, Howie, and Zussman; anthophyllites 9, 10, gedrites 5, 8, 9, 10. Rabbitt (1948), 5, 7, 8, 13, 16. Milton and Ito (1961), one analysis. Lall and Moorhouse (1969), 80, 112. Goroshnikov and Yur'yev (1965), Table 2, No. 3.

FIGS. 6, 7 and 8. All analyses appear in Figures 6 and 7, those in italics also appear in Figure 8. From Leake (1968): *83*, 87, 89, *97*, *109*, *110*, 112, 121, *122*, *124*, 126, *130*, 137, 142, *145*, *148*, *149*, 152, 158, 161, 162, *168*, 174, 175, 183, 186, 187, *190*, *192*, *203*, 206, 208, 212, 216, *217*, *219*, *220*, *221*, 225, *226*, 227, *228*, *233*, *235*, 236, *241*, 242, *252*, 258, 259, 265, 273, *276*, *277*, 281, *286*, 288, *290*, *297*, *300*, *302*, *306*, 308, *313*, 319, *326*, 328, *330*, *331*, 336, 337, 341, *343*, *373*, *381*, *382*, *388*, *394*, *397*, *401*, *403*, 404, *406*, 410, *411*, *413*, 417, 418, *422*, 427, *428*, 444, *447*, *450*, *455*, 458, *462*, *465*, *466*, *475*, *481*, *484*, *488*, *490*, *500*, *513*, *517*, *518*, *521*, 524, *530*, *534*, *540*, *546*, *549*, 553, *555*, *560*, 564, 570, 572, 573, *574*, *582*, 584, 586, 591, 596, *598*, *602*, *625*, *626*, 629, *630*, *634*, *637*, *647*, 653, *655*, 656, *660*, *716*, 719, *722*, *724*, 731, *734*, *737*, 742, 743, *745*, 747, *749*, *750*, *755*, *756*, *758*, *759*, *760*, *761*, *764*, *766*, 769, *772*, *780*, *782*, *783*, *787*, *788*, *791*, *794*, 795, 796, *798*, *801*, *803*, *808*, 809, *814*, *815*, 820, *821*, *824*, *827*, 829, *831*, 834, *838*, 844, 847, 848, *849*, *852*, 853, 854, *856*, 857, *861*, *867*, *868*, *872*, 876, *882*, *884*, *891*, *902*, *911*, 920, 928, 930, 932, 961, *965*, 966, *970*, *972*, *975*, 986, *992*, *1012*, *1014*, *1021*, *1022*, 1026, 1033, *1038*, *1041*, *1042*, 1046, *1056*, *1059*, 1069, 1074, *1075*, 1078, *1079*, *1080*, 1086, *1088*, 1090, 1095, *1098*, 1099, 1102, *1105*, *1107*, 1114, 1115, *1119*, 1121, 1123,

1125, 1127, *1128*, *1129*, *1131*, *1132*, 1134, *1135*, *1136*, *1148*, *1149*, *1152*, *1158*, 1159, 1166, *1170*, *1172*, *1175*, *1178*, *1179*, *1181*, *1194*, *1195*, *1199*, 1202, 1207, 1213, 1214.

From Binns (1965): *H2*, *H3*, *H4*, *H6*, *H10*, *H12*, *H18*, *H25*, *H26*, *H28*, *H29*, *H30*, *H34*, *H35*, *H36*, *H38*, *H39*, *H40*.

From Binns (1967): 1, 2, 3, 5.

From Dodge, Papike, and Mays (1968): *BCc-12*, *BCa-20*, MG-1, *MT-2*, *FD-13*, *2652*, *MT-4*, *WV-1*, *SL-32*, SL-18, *BCc-13*, *HL-9*, MG-3, *BP-2*, *BP-1*, *BP-6*, *FD-2*, FD-3, *MP-568*, KR, *CL-1*, 1970 (sic).

From Deer, Howie, and Zussman (1963): Edenites *1*, *2;* Tschermakitic Hornblende *10;* Richterites 1, 6, 7, 9; Kaersutite 10; Eckermannite-Arfvedsonite 1, 5, 13.

From Robinson and Jaffe (1969b) recalculated to 23(O): *N30X*, *6A9X*, 7A8BX, 7E8BX.

From Himmelberg and Papike (1968), hornblende-glaucophane pairs 29, 40, 50, 201.

From Henderson (1968): A2, A15, *A17*, A20, *A26*, *A28*, A31, *A76*, *A131*, A133, *A174*, A183, A226, *A16*, *A21*, A141, A177, *A439*.

FIG. 9. Klein (1968), wet analysis pairs 2-1, 2-2, 2-3, 2-5 recalculated to 23(O). Robinson and Jaffe (1969b): Table 2, N30X, 6A9X recalculated to 23(O); Table 4, QB27C-2A, QB27C-2B, J87D. Goroshnikov and Yur'yev (1965), Table 2, Nos. 1 and 3 recalculated to 23(O). Stout (1970c), 101A probe analyses of three coexisting amphiboles, anthophyllite recalculated to 23(O); gedrite recalculated assuming x/tet. Al=0.25; hornblende recalculated assuming 0.20 Na in $M(4)$.

FIG. 10. Wet analyses and probe analyses, Table 1, this paper. Probe analyses of anthophyllites and cummingtonites, Robinson and Jaffe (1969b, Table 4).

FIG. 11. For formulae with tetrahedral Al greater than 0.3 see Figs. 4 and 5 above. For formulae with tetrahedral Al less than 0.3: Deer, Howie, and Zussman (1963), anthophyllites 2, 6, 7, 8, 11; Rabbitt (1948), 26, 30, 32, 34, 40, 42, 43, 45, 46. Klein (1968), 2-1, 2-2. 3-1, 3-2, 3-3.